

AD-A066 374

NAVAL POSTGRADUATE SCHOOL MONTEREY CALIF  
INVESTIGATION OF PIPE FLOW INSTABILITY AND RESULTS FOR WAVE NUM--ETC(U)  
DEC 78 M J ARNOLD

F/G 20/4  
NUM--ETC(U)

UNCLASSIFIED

NL

1 OF 2

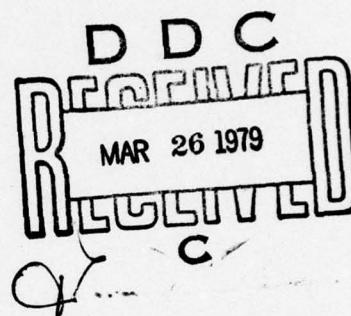
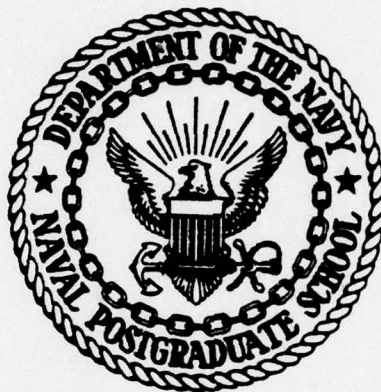
AD  
A066374



LEVEL *H*

(2)  
B.S.

NAVAL POSTGRADUATE SCHOOL  
Monterey, California



THESIS

INVESTIGATION OF PIPE FLOW INSTABILITY  
AND RESULTS FOR WAVE NUMBER ZERO

by

Michael James Arnold

December 1978

Thesis Advisor:

T. H. Gawain

Approved for public release; distribution unlimited.

79 03 26 065

AD A0 66374

DDC FILE COPY



UNCLASSIFIED

SECURITY CLASSIFICATION OF THIS PAGE (When Data Entered)

REPORT DOCUMENTATION PAGE		READ INSTRUCTIONS BEFORE COMPLETING FORM
1. REPORT NUMBER	2. GOVT ACCESSION NO.	3. RECIPIENT'S CATALOG NUMBER
4. TITLE (and Subtitle) Investigation of Pipe Flow Instability and Results for Wave Number Zero,		5. TYPE OF REPORT & PERIOD COVERED Master's Thesis December 1978
7. AUTHOR(s) Michael James Arnold		6. PERFORMING ORG. REPORT NUMBER
9. PERFORMING ORGANIZATION NAME AND ADDRESS Naval Postgraduate School Monterey, California 93940		8. CONTRACT OR GRANT NUMBER(s)
11. CONTROLLING OFFICE NAME AND ADDRESS Naval Postgraduate School Monterey, California 93940		10. PROGRAM ELEMENT, PROJECT, TASK AREA & WORK UNIT NUMBERS
14. MONITORING AGENCY NAME & ADDRESS (if different from Controlling Office) 123 p.		12. REPORT DATE December 1978
		13. NUMBER OF PAGES 122
		15. SECURITY CLASS. (of this report) Unclassified
		15a. DECLASSIFICATION/DOWNGRADING SCHEDULE
16. DISTRIBUTION STATEMENT (of this Report) Approved for public release; distribution unlimited.		
17. DISTRIBUTION STATEMENT (of the abstract entered in Block 20, if different from Report)		
18. SUPPLEMENTARY NOTES		
19. KEY WORDS (Continue on reverse side if necessary and identify by block number) Pipe Flow Instability		
20. ABSTRACT (Continue on reverse side if necessary and identify by block number) Past research by Harrison and Johnston on the stability of pipe flow yielded only tenuous results owing to errors in setup of the problem and in formulation of the complex axis boundary conditions. Recent advances in the formulation of these boundary conditions and application of generalized stability criteria allowed an accurate numerical solution to be made for angular wave number zero. The results show that flow for this case is characterized by certain		

DD FORM 1473

1 JAN 73

EDITION OF 1 NOV 68 IS OBSOLETE  
S/N 0102-014-6601

UNCLASSIFIED

SECURITY CLASSIFICATION OF THIS PAGE (When Data Entered)

254<sup>1</sup> 450

next page

elt

SECURITY CLASSIFICATION OF THIS PAGE (When Data Entered)

instabilities that have not been previously identified in linearized studies of this type.

A nonuniform computational mesh was developed which provided dramatic reductions in computational time on a limited basis.

Two data reduction programs were also developed to process and display data generated by the main program.

ADD TO for \_\_\_\_\_

\_\_\_\_\_ ☒ No Section  
\_\_\_\_\_ ☐ All Section ☐

DATE \_\_\_\_\_  
PRINTED NO. \_\_\_\_\_  
JUL 1 1967

BY \_\_\_\_\_  
DISTRIBUTION/ALTERNATE CODES  
Dist. \_\_\_\_\_ or SPECIAL

A

79 03 26 065

Approved for public release; distribution unlimited.

Investigation of Pipe Flow Instability  
and Results for Wave Number Zero

by

Michael James Arnold  
Lieutenant, United States Navy  
B.S., University of Idaho, 1969

Submitted in partial fulfillment of the  
requirements for the degree of

MASTER OF SCIENCE IN AERONAUTICAL ENGINEERING

from the

NAVAL POSTGRADUATE SCHOOL  
December 1978

Author

Michael James Arnold

Approved by:

T. H. Gawain

Thesis Advisor

Max F. Potter

Chairman, Department of Aeronautics

William M. Folkes  
Dean of Science and Engineering



### ABSTRACT

Past research by Harrison and Johnston on the stability of pipe flow yielded only tenuous results owing to errors in setup of the problem and in formulation of the complex axis boundary conditions.

Recent advances in the formulation of these boundary conditions and application of generalized stability criteria allowed an accurate numerical solution to be made for angular wave number zero. The results show that flow for this case is characterized by certain instabilities that have not been previously identified in linearized studies of this type.

A nonuniform computational mesh was developed which provided dramatic reductions in computational time on a limited basis.

Two data reduction programs were also developed to process and display data generated by the main program.



## TABLE OF CONTENTS

I.	INTRODUCTION -----	9
II.	THE VORTICITY TRANSPORT EQUATION -----	12
III.	NUMERICAL METHODS -----	17
IV.	RESULTS -----	25
	A. STABILITY -----	25
	B. PERTURBATION VELOCITY PLOTS -----	27
	C. STABILITY CONTOUR PLOTS -----	28
	D. NONUNIFORM MESH EFFECTS -----	29
	E. NUMERICAL ACCURACY -----	31
V.	CONCLUSIONS AND RECOMMENDATIONS -----	46
APPENDIX A:	DERIVATION OF VORTICITY TRANSPORT EQUATION COEFFICIENTS -----	48
APPENDIX B:	FINITE DIFFERENCE EQUATIONS -----	51
APPENDIX C:	NON-UNIFORM MESH -----	57
APPENDIX D:	DERIVATION OF PERTURBATION VELOCITIES -	65
COMPUTER PROGRAMS	-----	69
LIST OF REFERENCES	-----	121
INITIAL DISTRIBUTION LIST	-----	122

# LIST OF FIGURES

3-1	Finite Difference Mesh -----	18
3-2	Basic Composition of Coefficient Arrays and Vector of Unknowns -----	20
4-1	Normalized Perturbation Velocity -----	34
4-2	Normalized Perturbation Velocity -----	35
4-3	Normalized Perturbation Velocity -----	36
4-4	Normalized Perturbation Velocity -----	37
4-5	Normalized Perturbation Velocity -----	38
4-6	Stability Contour Plot -----	39
4-7	Stability Contour Plot -----	40
4-8	$\gamma^*$ Versus Number of Mesh Points, N -----	41
4-9	$\gamma^*$ Versus Number of Mesh Points, N -----	42
4-10	$\gamma^*$ Versus Mesh Parameter, Lambda -----	43
4-11	Normalized Perturbation Velocity -----	44
4-12	Normalized Perturbation Velocity -----	45
C-1	R versus $\eta$ for Four Selected Values of Lambda-Axis Offset -----	63
C-2	R versus $\eta$ for Four Selected Values of Lambda-Wall Offset -----	64

# TABLE OF SYMBOLS

C	Constant in non-uniform mesh functions given by equations (C-32) and (C-40)
$D, D^2, \dots$	Partial derivatives with respect to $r$ .
$D^*, D^{*2}, \dots$	Partial derivatives with respect to $\eta$ .
$e$	Base of natural logarithms.
$\bar{e}_x, \bar{e}_r, \bar{e}_\theta$	Unit vectors along the $x$ , $r$ and $\theta$ axes in cylindrical coordinates.
$F, G, H$	Components of the velocity vector potential defined in equation (2-6).
$f_{11}, f_{22}, \dots$	Coefficients of $D^*Q$ , $D^{*2}Q$ , ... in equations (C-9) through (C-12) as defined in equations (C-13) through (C-22).
$i$	$+\sqrt{-1}$ , the imaginary unit. Also used as an index in Section III and Appendix D.
$N$	The number of interior points in the finite difference mesh of Section III.
$O$	Symbol denoting the phrase "of order".
$Q$	The component of the velocity vector potential derived from the component $H$ by the change of variable, $H = rQ$ .
$R_e$	Reynolds number based on mean velocity and pipe radius.
$t$	Time.
$U$	The streamwise velocity in Pipe Poiseuille Flow as defined by equation (2-11).
$u, v, w$	Components of the complex perturbation velocity defined in equation (D-1).
$\bar{W}$	Complex vector potential of perturbation velocity defined in equation (D-2).
$x, r, \theta$	Cylindrical coordinates.
$\alpha$	$\alpha_R + i\alpha_I$ . Complex wave number of the perturbation in the $x$ -direction.



$\beta$	in. Complex wave number of the perturbation in the $\theta$ direction, where $n = 0, 1, 2, 3, \dots$
$\delta$	$1/(N+1)$ . The $r$ or $\eta$ increment in the finite difference approximations of the derivatives of $Q$ .
$\eta$	The independent variable replacing $r$ in the nonuniform mesh of Appendix C.
$\gamma$	$\gamma_R + i\gamma_I$ . Complex frequency of the perturbation.
$\bar{\Gamma}$	The vorticity transport equation expressed in abbreviated notation as defined in equation (2-7).
$\Gamma_x, \Gamma_r, \Gamma_\theta$	The components of $\bar{\Gamma}$ in cylindrical coordinates as defined in equation (2-7).
$\lambda$	Mesh offset parameter as defined in equations (C-32) and (C-40).
$\nabla$	Linear vector operator (nabla)
$\times$	Vector cross-product operator.
[ ]	Brackets enclosing a matrix.
{ }	Brackets enclosing a column vector.



## I. INTRODUCTION

The problem of finding an analytical solution to the pipe flow stability problem has been pursued actively ever since the classical experiments of Osborne Reynolds [10] about 100 years ago. Up to now, however, no investigation has been able to satisfactorily predict flow instabilities, although many approaches have been taken.

Salwen and Grosch [11] studied pipe flow with various angular wave numbers and sinusoidal streamwise perturbations and concluded that it was stable for all axial and angular wave numbers. Perturbations with exponential growth in space but a purely sinusoidal time variation were researched by Garg and Rouleau [2] and those with both exponential growth in space and in time by Gill [3]. Both concluded that the flows were stable.

Because of this inability of linear theory to account for experimental fact, explanations by Davey and Drazin [1] involving finite disturbances and by Huang and Chen [5] and Leite [7] involving conditions at the pipe entrance have been offered. While these investigations have indeed shown instabilities to exist, a completely general solution to the linear problem has never been achieved.

Recently a more general theory was presented by Harrison [4] and further investigated by Johnston [6]. These two studies, however, failed to produce conclusive results due

to mathematical errors in the problem setup and inadequate formulation of the boundary conditions at the axis. Gawain [9] has subsequently formulated the axis boundary conditions in a new way which corrects the previous discrepancies and promises further advances.

For angular wave number,  $n$ , equal to zero, radical simplifications result in the governing equations (Section II), indicating that this case should be approached first. This investigation centers on that case.

Preliminary checks using the computer program of Ref. 6 revealed that, of the two eigenfunctions,  $G$  and  $H$ , which occur in this problem and which are uncoupled for  $n = 0$ , the latter appeared to be the more critical. Hence the present research was arbitrarily restricted to investigation of the stability of eigenfunction  $H$ . A similar study of the other eigenfunction,  $G$ , for  $n = 0$  remains to be completed at some future time. Comparable calculations for other wave numbers ( $n = 1, 2, 3, \dots$ ) also remain to be accomplished in the future. Extensive and systematic calculations of this type will be essential to provide the factual basis for a comprehensive theory of pipe flow stability.

Reverting to the case at hand, eigenfunction  $H$  for wave number  $n = 0$ , we note that the program of Ref. 6 was rewritten for this case, incorporating the newly formulated boundary conditions of Ref. 9. In addition, a new, generalized stability criteria was adopted. Moreover, a new technique was introduced which allows the use of nonuniform meshes to reduce computational time.

Lastly, two data reduction programs were written to process data produced by the main investigative program.



## II. THE VORTICITY TRANSPORT EQUATION

Although a complete treatment of this subject is contained in Appendix A of Ref. 4 and further addressed in Ref. 6 and Ref. 9, it is felt that a brief overview is still required here to maintain continuity with previously referenced works. This discussion is an abbreviated version of Section II of Ref. 6.

Laminar flow of an incompressible fluid of constant viscosity is governed by the Navier-Stokes equation and the continuity equation. Taking the curl ( $\nabla \times$ ) of the Navier-Stokes equation and introducing a perturbation velocity ( $\bar{v}$ ) and vorticity ( $\bar{\omega}$ ) gives the vorticity transport equation which is equation (A-10) of Appendix A, Ref. 4.

Expressing this equation in terms of the complex velocity vector potential,  $\bar{W}$ , gives

$$W(x, r, \theta, t) = (\bar{e}_x F(r) + \bar{e}_r G(r) + \bar{e}_\theta H(r)) e^X \quad (2-1)$$

where

$$X = \alpha x + \beta \theta + \gamma t \quad (2-2)$$

and

$$\bar{v} = \nabla \times \bar{W} \quad (2-3)$$



$$\bar{\omega} = \nabla \times \bar{v}. \quad (2-4)$$

It should also be noted that, as shown in part one of Appendix G in Ref. 4,  $\alpha$  and  $\gamma$  are complex while  $\beta$  is a purely imaginary quantity defined by

$$\beta = i n \quad n = 0, 1, 2, \dots \quad (2-5)$$

When expressed in the form of equation (2-1), the vorticity transport equation becomes three simultaneous fourth-order differential equations of the form

$$\begin{aligned} & [M_4] \begin{Bmatrix} D^4 F \\ D^4 G \\ D^4 H \end{Bmatrix} + [M_3] \begin{Bmatrix} D^3 F \\ D^3 G \\ D^3 H \end{Bmatrix} + [M_2] \begin{Bmatrix} D^2 F \\ D^2 G \\ D^2 H \end{Bmatrix} \\ & + [M_1] \begin{Bmatrix} DF \\ DG \\ DH \end{Bmatrix} + [M_0] \begin{Bmatrix} F \\ G \\ H \end{Bmatrix} - \gamma ([N_2] \begin{Bmatrix} D^2 F \\ D^2 G \\ D^2 H \end{Bmatrix} \\ & + [N_1] \begin{Bmatrix} DF \\ DG \\ DH \end{Bmatrix} + [N_0] \begin{Bmatrix} F \\ G \\ H \end{Bmatrix}) = \begin{Bmatrix} 0 \\ 0 \\ 0 \end{Bmatrix} \end{aligned} \quad (2-6)$$

Equations (2-5) may be further expressed in the abbreviated form

$$\bar{\Gamma} = \begin{Bmatrix} \bar{\Gamma}_x \\ \bar{\Gamma}_r \\ \bar{\Gamma}_\theta \end{Bmatrix} = \begin{Bmatrix} 0 \\ 0 \\ 0 \end{Bmatrix} \quad (2-7)$$

where  $\bar{\Gamma}$  appears to be a set of three coupled equations in the components of  $\bar{W}$ . As given in Appendix B of Ref. 4, equations (2-7) actually represent only two independent conditions and by an appropriate linear combination of  $\Gamma_x$  and  $\Gamma_\theta$ , equations (2-6) can be expressed as a set of two equations in three unknowns. The appropriate linear combination is given in Appendix B of Ref. 4 and yields the set of equations

$$\begin{aligned} \Gamma_r &= 0 \\ -\frac{in}{r} \Gamma_x + \alpha \Gamma_\theta &= 0. \end{aligned} \quad (2-8)$$

Except for the case where  $n$  is equal to zero, equations (2-8) do not uncouple. The linear combination given by the second of equations (2-8) does, however, reduce the highest order derivative of  $G(r)$  in equations (2-6) to second order. Appendix C of Ref. 4 illustrates the redundancy of the three components of  $\bar{W}$ , allowing one of these components to be arbitrarily set to zero for all  $r$ . The maximum benefits of equations (2-8) are obtained if

$$F(r) = 0 \quad (2-9)$$

Incorporating equations (2-8) and (2-9) into equations (2-6) results in the form

$$\begin{aligned}
 & [M'_4] \begin{Bmatrix} D^4_G \\ D^4_H \end{Bmatrix} + [M'_3] \begin{Bmatrix} D^3_G \\ D^3_H \end{Bmatrix} + [M'_2] \begin{Bmatrix} D^2_G \\ D^2_H \end{Bmatrix} \\
 & + [M'_1] \begin{Bmatrix} DG \\ DH \end{Bmatrix} + [M'_0] \begin{Bmatrix} G \\ H \end{Bmatrix} - \gamma ([N'_2] \begin{Bmatrix} D^2_G \\ D^2_H \end{Bmatrix} \\
 & + [N'_1] \begin{Bmatrix} DG \\ DH \end{Bmatrix} + [N'_0] \begin{Bmatrix} G \\ H \end{Bmatrix}) = \begin{Bmatrix} 0 \\ 0 \end{Bmatrix} \quad (2-10)
 \end{aligned}$$

where the coefficient matrices are given by equations (2-10) through (2-17) of Ref. 6. It is appropriate to note that these same coefficient matrices appear in Ref. 9, equations (A1) through (A9), in a slightly different form resulting from the substitutions

$$U = 2(1 - r^2) \quad (2-11)$$

$$t = \alpha^2 + \frac{\beta^2}{r^2} \quad \text{and} \quad (2-12)$$

$$T = \alpha U - \frac{1}{R_e} \left( \alpha^2 + \frac{\beta^2}{r^2} \right) . \quad (2-13)$$

As discussed in the previous section, the case where

$$\beta = \text{in} , \quad n = 0 \quad (2-14)$$



leads to great simplifications in equations (2-10), (2-12) and (2-13). In particular, equations (2-10) uncouple and allow an independent investigation of either H or G. As a result of the findings discussed in Section I, it was decided to explore the function H only. This reduced equation (2-10) to that of equation (A-6) of Appendix A, which is a linear, homogeneous fourth order differential equation in  $H(r)$ .



### III. NUMERICAL METHODS

Substituting the change of variable  $H = rQ$  as given in equation (A-1) and the coefficients defined in equations (A-11) through (A-18) into the vorticity transport relation, equation (A-6), gives the expression

$$\begin{aligned} M_4 D^4 Q + M_3 D^3 Q + M_2 D^2 Q + M_1 DQ + M_0 Q \\ - \gamma [N_2 D^2 Q + N_1 DQ + N_0 Q] = 0, \end{aligned} \quad (3-1)$$

which is a homogeneous fourth order differential equation in  $Q(r)$ . The boundary conditions for this case are derived in detail in Ref. 9 as

$$\begin{aligned} Q(1) &= 0 \\ DQ(1) &= 0 \\ DQ(0) &= 0 \\ D^3 Q(0) &= 0. \end{aligned} \quad (3-2)$$

The boundary finite difference equations derived in Appendix B from equations (3-2), along with the standard central difference equations given in Ref. 6, allow the function  $Q(r)$  to be approximated by a finite number of discrete unknowns. As shown by Figure 3-1 below, the non-dimensionalized radius of the pipe is divided into a one-dimensional

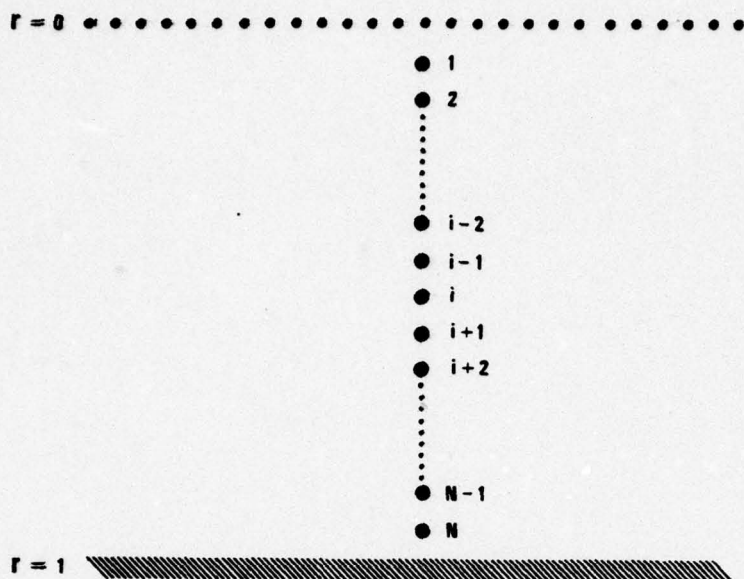


Figure 3-1 Finite Difference Mesh

computational mesh consisting of  $N$  interior points,  $N+1$  intervals, and  $N+2$  total points, including the boundary points at  $r = 1$  and  $r = 0$ . As will be discussed later, the spacing between these points may or may not be uniform. For the uniform case, the spacing is defined by

$$\delta = 1/(N+1) . \quad (3-3)$$

For the nonuniform case, a change of independent variable is performed. The spacing of the new independent variable,  $\eta$ , is still given by equation (3-3).

With a nonuniform mesh, the points shown in Figure 3-1 will be concentrated near the axis or near the wall according

to the type of offset specified. These effects are discussed in detail in Section IV.

Substitution of the finite difference equations of Appendix B into equation (3-1) results in a set of  $N$ , linear, algebraic difference equations in terms of the unknown value of  $Q$  at each of the  $N$  interior points of the computational mesh. Since each of these equations is of the form of a linear combination of the  $i$ th, central, point and the two, three or four adjacent points (depending on the order of the derivative being approximated), this system of equations consists of a coefficient array multiplying a vector containing the unknown value of the function  $Q$  at each of the  $N$  interior points. This technique allows the problem to be converted into an eigenvalue problem of the form

$$[X] \{Q\} - \gamma [Y] \{Q\} = 0 \quad (3-4)$$

with the basic composition of the arrays  $[X]$  and  $[Y]$  and the vector  $\{Q\}$  as illustrated in Figure 3-2 below.

It should be noted at this point that Figure 3-2 differs somewhat from the normal finite difference banded matrix in the first two rows and last row because of the method of deriving the finite difference approximations at the boundaries. Additionally, the order of the  $N$  unknowns has been reversed from that of Ref. 6. This was done to conform to standard matrix notation.



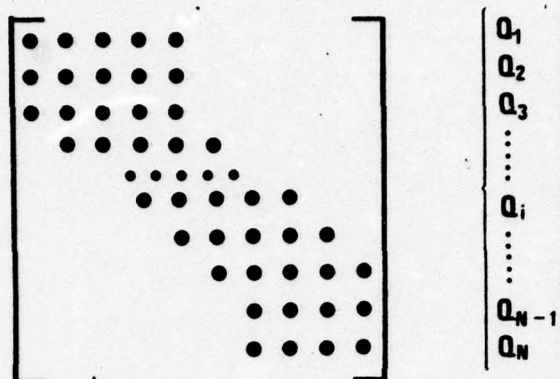


Figure 3-2 Basic Composition of Coefficient Arrays and Vector of Unknowns

This array is established by the subroutine MSET2 in conjunction with the subroutine MSET1 and function subprograms CQM1E1 and CQM2E1, which compute the numerical value for each element in the array. Subroutine MSET1 provides the coefficients given by equations (A-11) through (A-18) of Appendix A or by equations (C-24) through (C-31) if a nonuniform mesh is specified. Function CQM1E1 then computes the values for each of the elements of array [X] in equation (3-4) using the coefficients passed from subroutine MSET1 in vector CQM1. Function subprogram CQM2E1 performs the same function for matrix [Y] in equation (3-4) using the coefficients passed in vector CQM2.

The solution of the eigenvalue problem as formulated to this point is carried out by the controlling subroutine of program PIPE0, subroutine STAB, by the following steps:

- 1) Subroutine MSET2 is called twice to set up the coefficient matrices [X] and [Y] of equation (3-4).

- 2) Subroutine CDMTIN is then called to invert matrix  $[Y]$ , the second coefficient array in equation (3-4). CDMTIN was obtained from the IBM Library routine CMTRIN by modifying it to accept double precision arrays.
- 3) Both coefficient arrays,  $[X]$  and  $[Y]$ , are then pre-multiplied by  $[Y]^{-1}$ . Since multiplication of an array by its inverse invariably results in the identity matrix,  $[I]$ , only the product  $[Y]^{-1}[X]$  is computed using subroutine MULM. This converts the eigenvalue problem of equation (3-4) to the more conventional form

$$([Z] - \gamma[I])\{Q\} = 0 \quad (3-5)$$

where

$$[Z] = [Y]^{-1}[X] \quad (3-6)$$

- 4) Since all programs currently available for solving equations (3-5) require that the real and imaginary parts of the elements of  $[Z]$  be presented in separate arrays, subroutine DSPLIT is called to accomplish this.
- 5) The eigenvalues and eigenvectors of equations (3-5) are computed using subroutines EBALAC, EHESSC, ELRH2C and EBBCKC which are available through the International

Math and Statistics Library. Subroutine EBALAC balances matrix [Z] by equalizing the exponents of all terms. The details of this transformation are retained for later use. The balanced matrix is then passed to subroutine EHESSC where it is reduced into the complex upper Hessenberg form. Subroutine ELRH2C then solves for the eigenvalues and eigenvectors. To transform the eigenvectors back into the original unbalanced form, EBBCKC is finally called using information passed from subroutine EBALAC.

For each solution, subroutine STAB determines the least stable eigenvalue (largest algebraic value) and then writes the values of  $N$ ,  $R_e$ ,  $\alpha_R$ ,  $\alpha_I$ ,  $\lambda$ ,  $\gamma_{RL}$ ,  $\gamma_{IL}$  and KSET to file FT02F001. The eigenvector corresponding to the least stable eigenvalue is also written to FILE FT02F001 when MODENO is set equal to one.

Control of subroutine STAB is accomplished by the main program, PIPE0. This program is a time-sharing (CP/CMS) program. Modes one and three compute the stability of the flow for a given set of input conditions. Mode one writes the least stable eigenvector to FILE FT02F001 while this output is inhibited when MODENO is set equal to three. To generate data for program EIGFCN, program PIPE0 must be run with MODENO equal to one.



Mode two operation generates a grid of stability values (stability map) based on parameters read in from FILE FT01F001. Due to the long run time in this mode, only small meshes can be generated under CP/CMS. Longer runs must be accomplished under batch, with changes to the program as specified in the comments section. Data is output to file FT03F001 when MODENO is equal to two and is compatible with program STBCONT.

The plotting programs EIGFCN and STBCONT were used to process the data generated by program PIPE0 in modes one and three, respectively. Program EIGFCN generates normalized plots of the perturbation velocity,  $u$ , as a function of radius,  $r$ . The perturbation velocities generated in accordance with Appendix D were normalized in two steps. First the perturbation velocity of largest magnitude was determined. Letting this velocity be termed  $u_c$ , a normalizing constant producing unit magnitude and zero phase angle in  $u_c$  was found in the following manner:

If

$$u_c = u_{RC} + iu_{IC} , \quad (3-7)$$

then

$$Cu_c = 1 + i(0) \quad (3-8)$$

where C is the normalizing constant. Thus,

$$C = \frac{1}{u_{RC} + i u_{iC}} = \frac{u_{RC} - u_{iC}}{(u_{RC}^2 - u_{iC}^2)} \quad (3-9)$$

$$= \frac{\bar{u}_C}{|u_C|^2} \quad (3-10)$$

where  $\bar{u}_C$  is the complex conjugate of  $u_C$ .

The nondimensionalized radius values were taken directly from the data cards for uniform meshes or computed from equations (C-32) or (C-40) in the case of a nonuniform mesh.

Program STBCONT plots the stability contours against  $\alpha_R$  and  $\alpha_I$ . The stability map generated by program PIPE0 is searched columnwise and rowwise for sign changes for each of the three stability criteria discussed in Section V and Ref. 9. The points are then plotted, producing contours of incipient, critical and fully developed instability and areas that denote stable flow and subcritical, supercritical and hypercritical instability.

Both programs, EIGFCN and STBCONT, utilize the NPS VERSATEC plotter, certain built-in VERSATEC subroutines, and subroutine PLOTG. These routines are only accessible when running under FORTCLGW.

#### IV. RESULTS

##### A. STABILITY

Since an understanding of the term stability is necessary to interpret the results of this investigation, a brief discussion is presented here. A complete discussion of the generalized criteria of stability is given by Gawain [9].

The characteristics of the flow for the case  $n = 0$  are set by the parameters  $R_e$  and  $\alpha$ . For fixed values of these parameters, the solution of equations (3-5) is a set of  $N$  eigenvalues,  $\gamma$ , and their corresponding eigenvectors,  $Q$ . As can readily be seen from equation (2-1), the value of the real part of the complex eigenvalue  $\gamma$  will determine the growth or decay rate in time of the perturbation. Since positive values of the real part of  $\gamma$  represent an exponential growth rate in time, the most important  $\gamma$  is the one having the largest algebraic value for its real part. This root is termed the least stable root and will be represented by the symbol  $\gamma_{RL}$ . As the stability represented by  $\gamma_{RL}$  is that seen by a fixed observer, it is not the most general criterion. As derived in Ref. 9, a more appropriate stability criterion is that based on an axis system moving at the average volumetric velocity of the flow. This criteria is termed  $\gamma_{RL}^*$  and is defined by Ref. 9 as



$$\gamma_{RL}^* = \gamma_{RL} + \alpha_R . \quad (4-1)$$

For this and subsequent discussions, the subscript will be dropped and  $\gamma^*$  will refer to the quantity defined by equation (4-1). Three stability cases arise from this equation. The first is termed incipient instability and is defined by

$$\gamma^* = -|\alpha_R| . \quad (4-2)$$

The second case, termed critical instability, is given by

$$\gamma^* = 0 \quad (4-3)$$

and, lastly, the case termed fully developed instability is said to exist when

$$\gamma^* = +|\alpha_R| . \quad (4-4)$$

The transition from stable flow to fully developed instability is progressive and several distinct stages are given in Ref. 9 to describe this transition. The region from incipient to critical instability is termed subcritical instability, that from critical instability to fully developed instability is called supercritical instability while that beyond fully developed instability is termed hypercritical instability.

## B. PERTURBATION VELOCITY PLOTS

Initial investigation of the function  $Q$  was centered around plotting its appearance in the region of interest. A Reynolds number of 1150 (2300 based on diameter) was chosen as this value is generally accepted as the nominal value for transition to turbulent flow. The value of  $\alpha$  was set at  $-0.5 + i 10.0$  for the major part of the investigation as preliminary checks revealed that supercritical instabilities were present for this value. A secondary Reynolds number of 4000 was chosen to show trends.

The quantity chosen as the most realistic and representative of the eigenfunction  $Q$  is the axial perturbation velocity,  $u$ . This quantity was derived from the elements of the least stable eigenvector as outlined in Appendix D. Initially,  $R_e$  and  $\alpha_I$  were held fixed and  $\alpha_R$  was varied over a range of positive and negative values. For values of  $\alpha_R$  below about two, the normalized perturbation velocity was found to have all activity near the axis with a decay essentially to zero by  $r = 0.3$ . A typical plot of  $u$  versus  $r$  for an  $\alpha_R$  in this range is shown in Figure 4-1. When  $\alpha_R$  was made sufficiently positive, the plot changed significantly in both appearance and region of activity. Figure 4-2 shows a plot of  $u$  for  $\alpha_R = 2.5$ . The activity can now be seen to be concentrated near the wall, with most of the activity occurring at  $r$  values greater than 0.7.

Although no particular relationship between the nature of  $u$  and the stability of the flow was evident or expected,

the plots were nevertheless valuable as indicators for various parameters involved in the investigation.

First, as can be seen by the differences in Figures 4-1 and 4-2, the plots were ideal indicators of changes in the nature of the function  $Q$ . Secondly, the adequacy of the mesh could be directly observed by noting the number of points defining the curves in regions of high activity. Figures 4-3, 4-4 and 4-5 show the same conditions as Figure 4-1 but with decreasing number of mesh points,  $N$ . Lastly, the effects of nonuniform meshes could be observed as will be discussed later in this section.

#### C. STABILITY CONTOUR PLOTS

The principal results of this investigation are shown in Figures 4-6 and 4-7. Although these two figures pertain to only a limited portion of the complex  $\alpha$  plane, they do represent a significant advance in the investigation of pipe flow stability. As can be seen in these figures, the flow is characterized by regions of differing stability, ranging from stable through supercritical instability. Note that these two figures correspond to Reynolds numbers of 1150 and 4000, respectively. This is a result that has not, to this writer's knowledge, been heretofore achieved by a linearized analysis of fully developed pipe flow. The figures also show that, as has been born out by previous investigations, flow for purely sinusoidal oscillations ( $\alpha_R = 0$ ) is stable. Additionally, a comparison of Figures 4-6



and 4-7 shows the effect of Reynolds number on the flow stability. It is clear from this comparison that an increase in Reynolds number reduces the size of the stable regions in the complex  $\alpha$  plane; in other words, stability decreases with increasing Reynolds number. This trend agrees with our general experience pertaining to fluid flow. Lastly, the effect of the real and imaginary parts of the wave number  $\alpha$  can readily be seen. For  $\alpha_R$ , increasingly negative values produce successively greater levels of instability. While a contour plot was not produced for positive values of  $\alpha_R$ , point checks of stability in this region suggest that somewhat similar contours exist in the right half-plane also. For  $\alpha_I$ , increasing values produce increasing stability. This effect is also more pronounced at the lower Reynolds number.

#### D. NONUNIFORM MESH EFFECTS

One of the difficulties in this investigation was the relatively long computing time required to obtain an accurate solution, especially when operating under CP/CMS (time-sharing). The major factor controlling computing time was the number of interior mesh points,  $N$ . As an example, an increase in  $N$  of 50 percent resulted in a fourfold increase in computing time. Therefore, the desired objectives of rapidity and accuracy were in direct conflict. Additionally, follow-on investigations for values of angular wave number  $n$  other than zero involve matrices twice the order required for this case because of the coupling of equations (2-8).

For these reasons, a nonuniform mesh was developed to obtain increased accuracy at lower values of  $N$ . The nature of the velocities as seen in Figures 4-1 and 4-2 shows that a high degree of resolution in the computational mesh is only required in the vicinity of the axis ( $\alpha_R$  less than about 2) or the wall ( $\alpha_R$  greater than about 2). It was therefore theoretically possible to redistribute the points at moderate values of  $N$  to attain resolutions equivalent to much finer (and more time-consuming) uniform meshes.

As can be seen from Figures 4-8 and 4-9, the value of  $\gamma^*$  varies with the number of mesh points,  $N$ . Theoretically, each of these curves would approach some limiting value if  $N$  were increased without bound, and it is this theoretical limit that represents the required solution. In practice, it is adequate to approximate the unknown limit by a point that lies on the relatively flat portion of the curve at a value of  $N$  which is practically attainable and which does not involve a prohibitively long computing time. It has been found in this investigation that  $N = 79$  fulfills these conditions.

The conversion to a nonuniform mesh involved a change of independent variable and the introduction of an analytical function to control the distribution of the mesh points. The details of these steps are given in Appendix C. By varying the mesh offset parameter,  $\lambda$ , it was possible to vary  $\gamma^*$  over a wide range. To determine when the high

accuracy solution ( $N = 79$ ) and the nonuniform solutions were approximately equal,  $\gamma^*$  was plotted versus  $\lambda$  for fixed values of  $R_e$ ,  $\alpha$  and  $N$  with the value of  $\gamma^*$  for  $N = 79$  as a reference. Figure 4-10 shows a plot of this type for  $N = 31$ . The appropriate value of  $\lambda$  can be seen to be approximately 1.1. Figure 4-11 is the perturbation velocity plot of the solution for  $N = 31$  and  $\lambda = 1.1$  for the same  $R_e$  and  $\alpha$  as Figure 4-1. Note that the  $\gamma^*$  values are equal for these two figures. While the resolution of Figure 4-11 is not quite as fine as that of Figure 4-1, a comparison of Figure 4-11 with Figure 4-5 makes the improved resolution obvious. Figures 4-2 and 4-12 are similar to Figures 4-1 and 4-11 except that a wall offset was used. Note that for this case  $\lambda = 1.2$ , which points to a drawback of the nonuniform mesh, that of dependence on input conditions. While a check of  $\lambda$  dependence on  $\alpha$  was not made, it most probably exists. There is also, however, the possibility that for small regions of the complex  $\alpha$  plane, the variations in  $\lambda$  are small enough to allow an average value of  $\lambda$  to be nearly optimum for the entire region. While not used for the main results of this study, the method as developed here may well prove to be of maximum utility in follow-on investigations of higher angular wave numbers.

#### E. NUMERICAL ACCURACY

To ensure that the solutions presented here were of sufficient accuracy, two separate checks were made. The



first,  $\gamma^*$  dependence on  $N$ , is the most commonly used criterion.

For a solution to be accurate, it should be virtually independent of mesh fineness, that is, of  $N$ . The required magnitude of  $N$  for an accurate solution was found by plotting  $\gamma^*$  against  $N$ . Figures 4-8 and 4-9 both show that the solution is well converged for  $N = 79$  at Reynolds numbers of 1150 and 4000, as  $\gamma^*$  changes by only .001 to .003 from  $N = 31$  to  $N = 79$  for both values of Reynolds number.

The second verification of the solution, so obvious that it is sometimes overlooked, involves simply substituting the numerical solution (least stable eigenvector) into the governing equation to ensure that it is indeed being satisfied. A short program was independently written to check the finite difference representations of equation (3-1) at the first and last interior stations and at a mid-radius station. Initial checks of numerical solutions yielded unsatisfactory results and led to the discovery of various programming errors. In particular, it was discovered that four double precision constants in the finite difference approximations were lacking the required "D0" exponent. Elimination of these seemingly trivial errors resulted in a surprising four order-of-magnitude improvement in the accuracy of the solution, with the left side of equation (3-1) improving from order  $10^{-4}$  to order  $10^{-8}$ .

It is instructive to note at this point that the order of magnitude of the left side of equation (3-1) is not the

true measure of its satisfaction. A more correct procedure is to compare this value with the largest term in the equation. When examined from this viewpoint, the relative error for solutions at  $R_e = 1150$  and  $R_e = 4000$  are found to be of order  $10^{-11}$  to  $10^{-12}$ , a very satisfactory result.

Therefore, by these results, the solutions presented here are both virtually independent of  $N$  and satisfy the governing differential equation to a high degree. The efforts expended to reach these conclusions were well worth the result and also point out that attention to detail is fundamental to accurate numerical results.

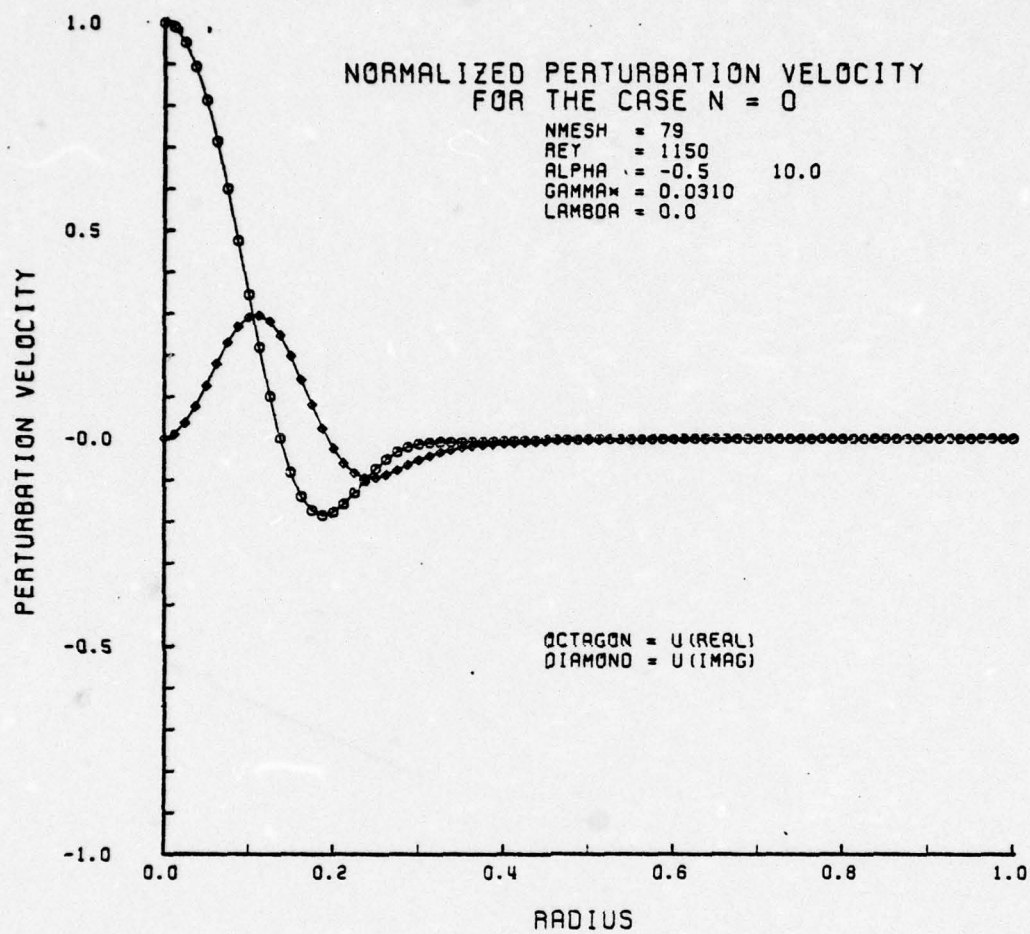


FIGURE 4-1



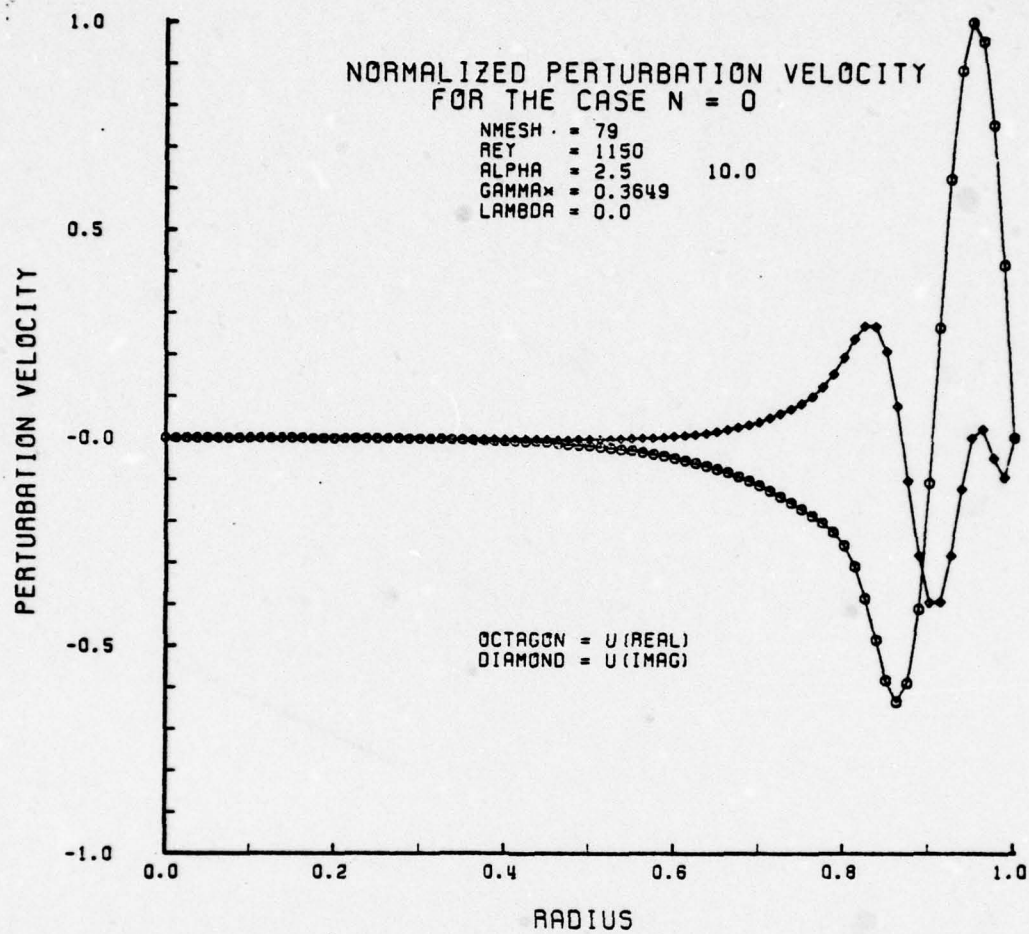


FIGURE 4-2

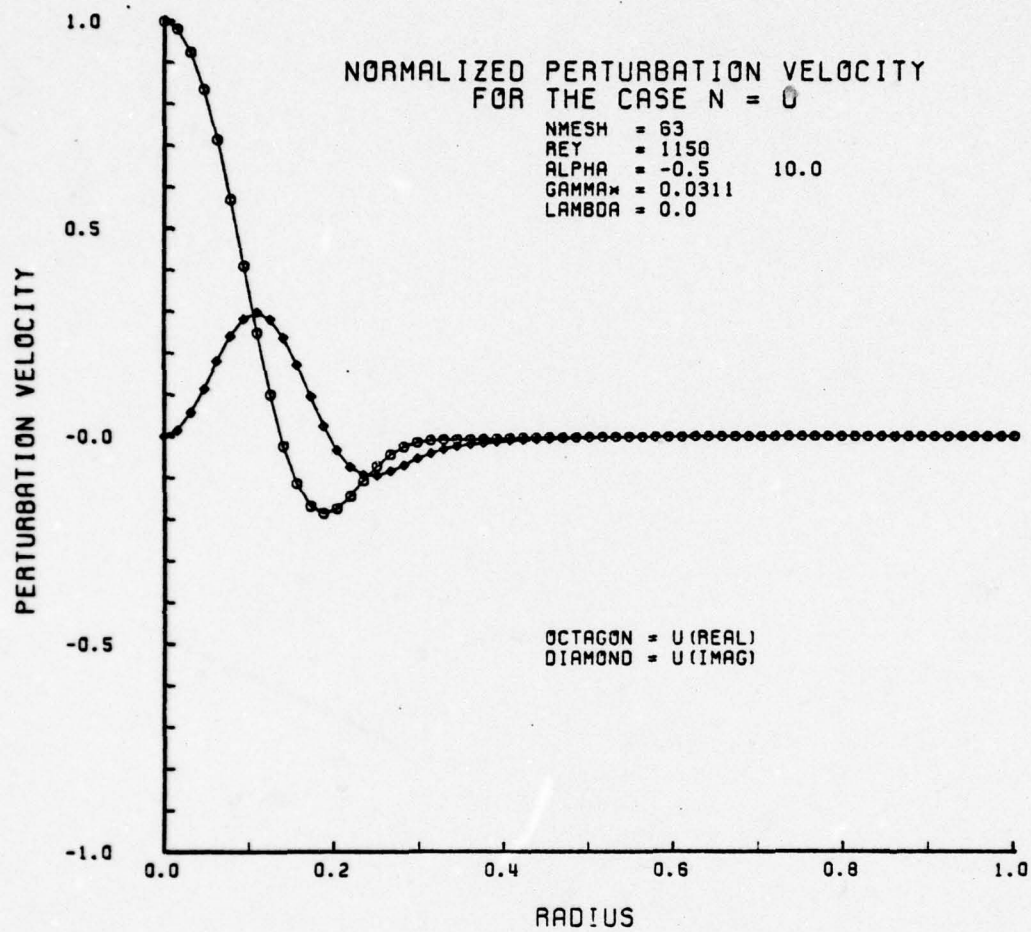


FIGURE 4-3

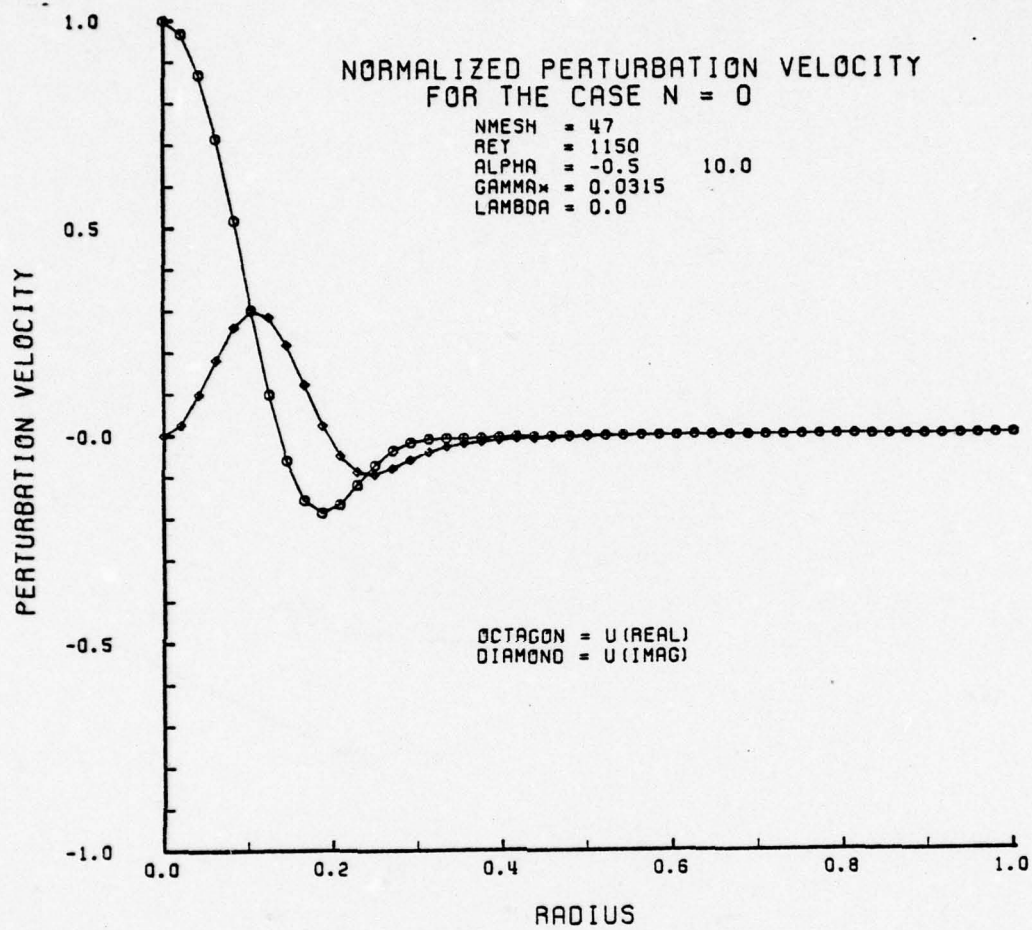


FIGURE 4-4



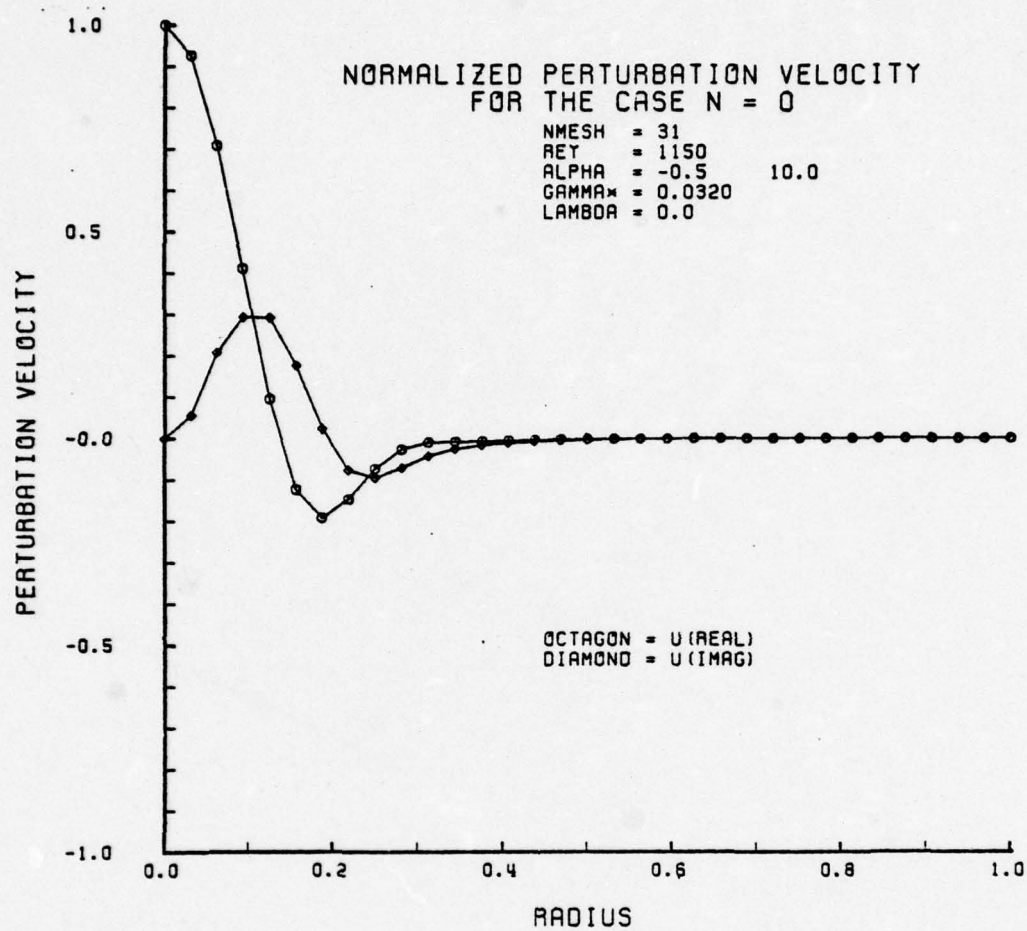


FIGURE 4-5

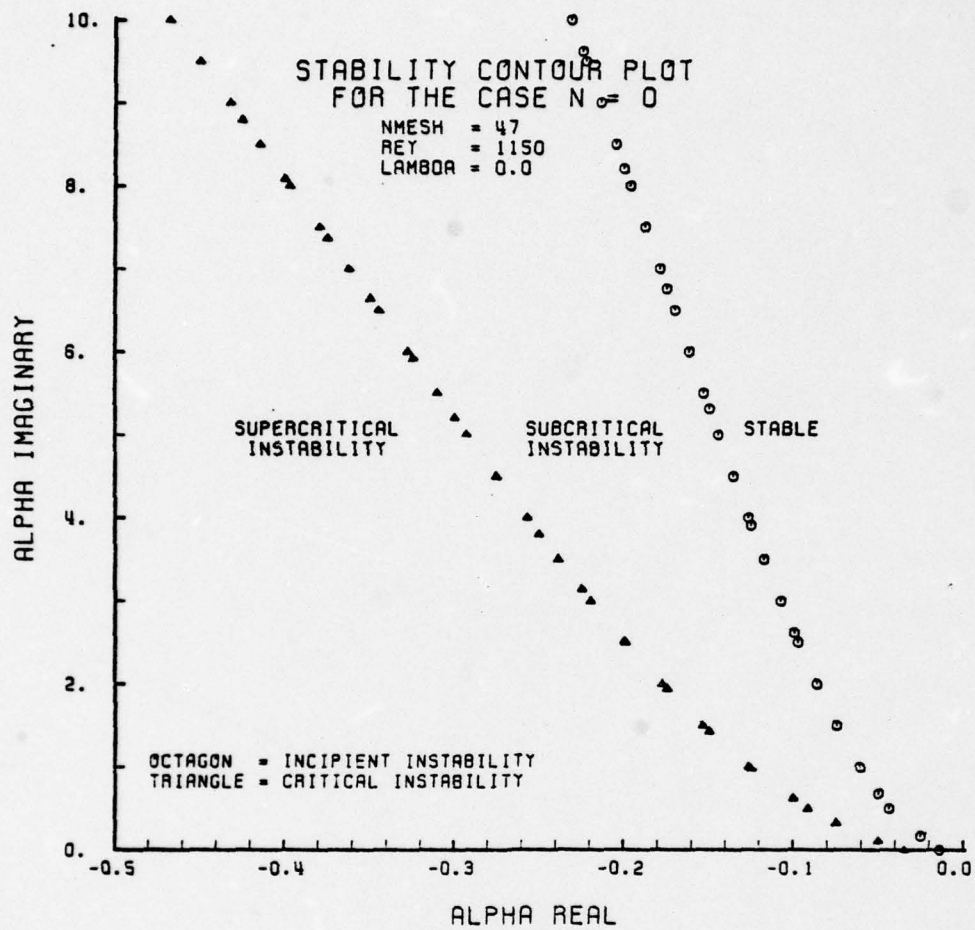


FIGURE 4-6

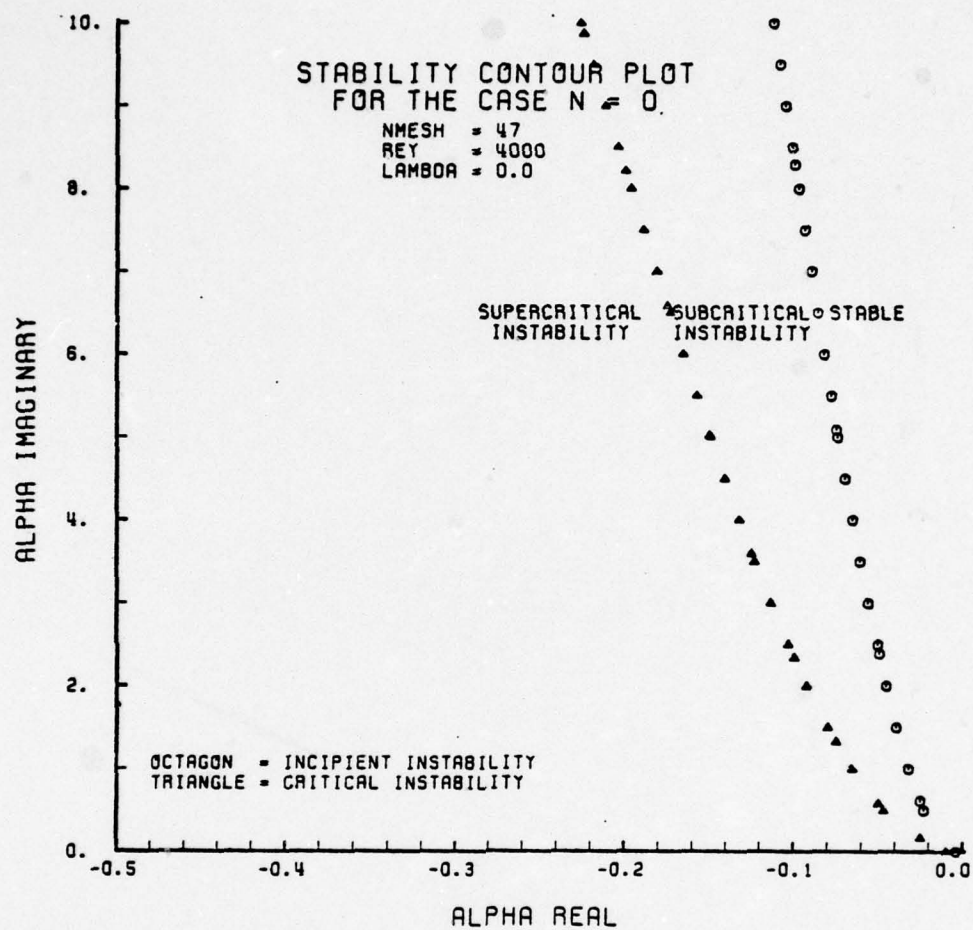


FIGURE 4-7



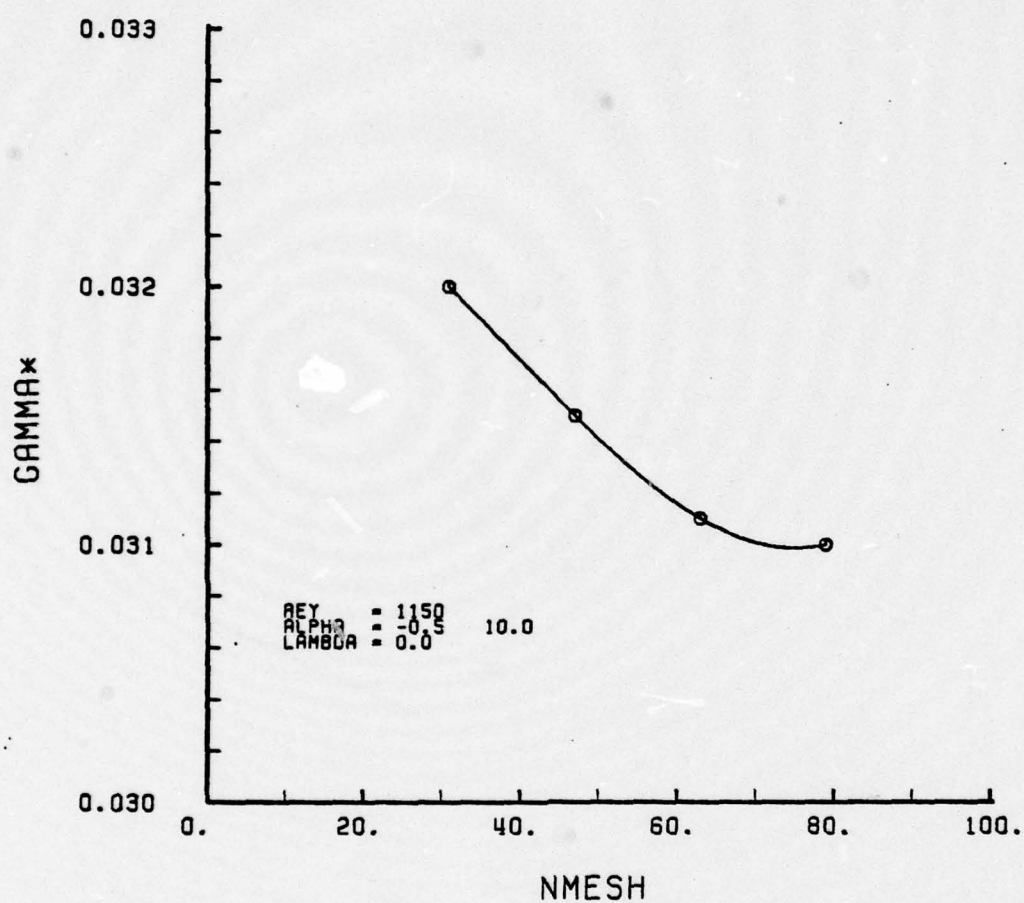


FIGURE 4-8.  $\gamma^*$  Versus Number of Mesh Points, N.

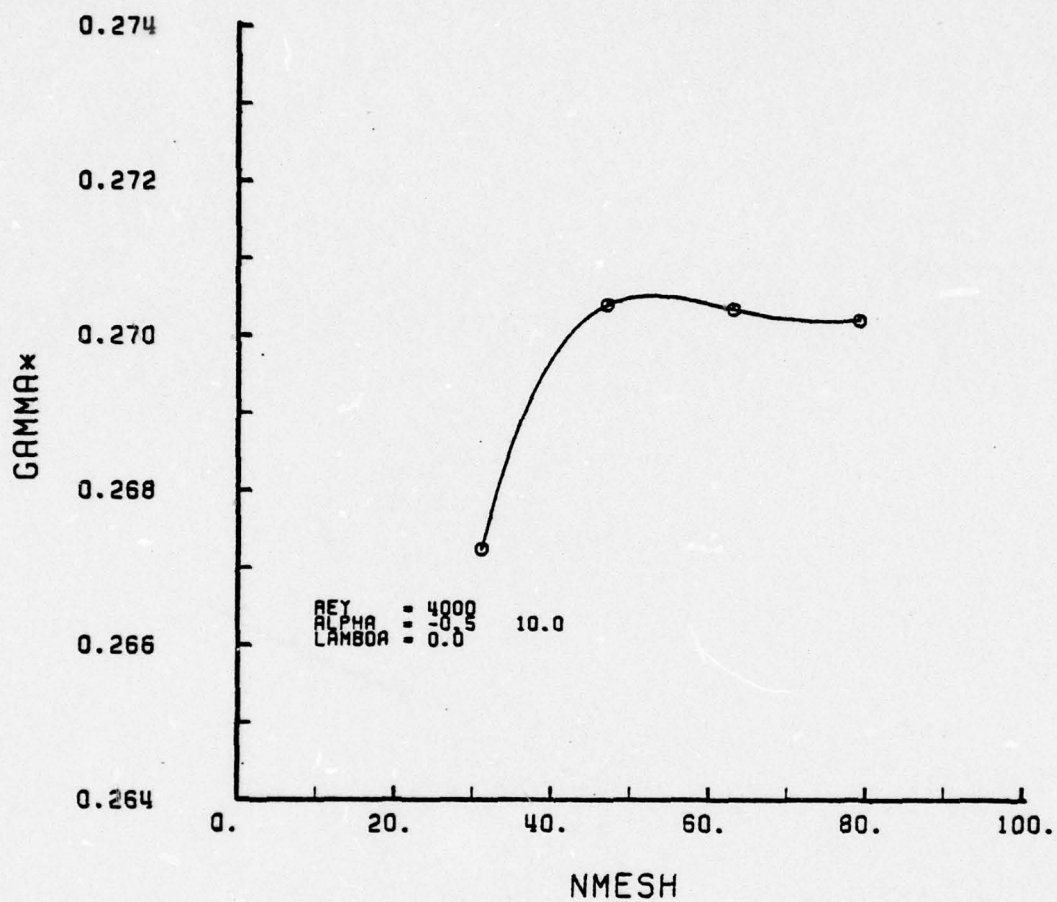


FIGURE 4-9.  $\gamma^*$  Versus Number of Mesh Points, N.

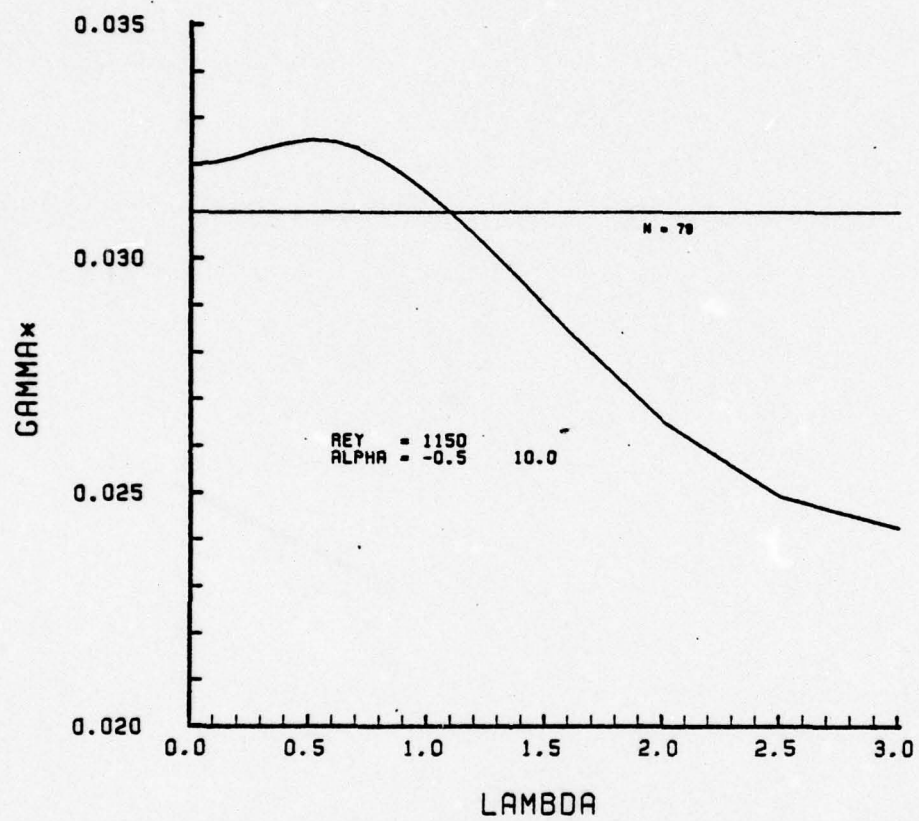


FIGURE 4-10.  $\gamma^*$  Versus Mesh Parameter, Lambda



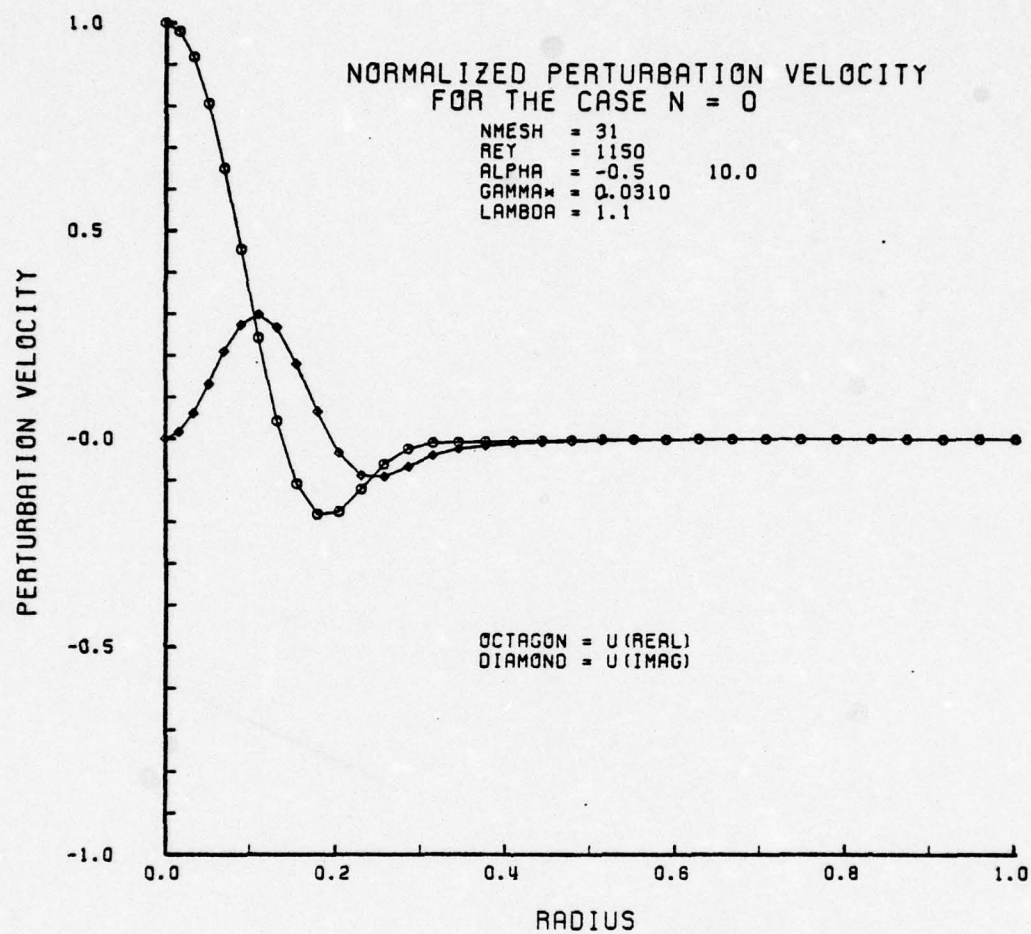


FIGURE 4-11

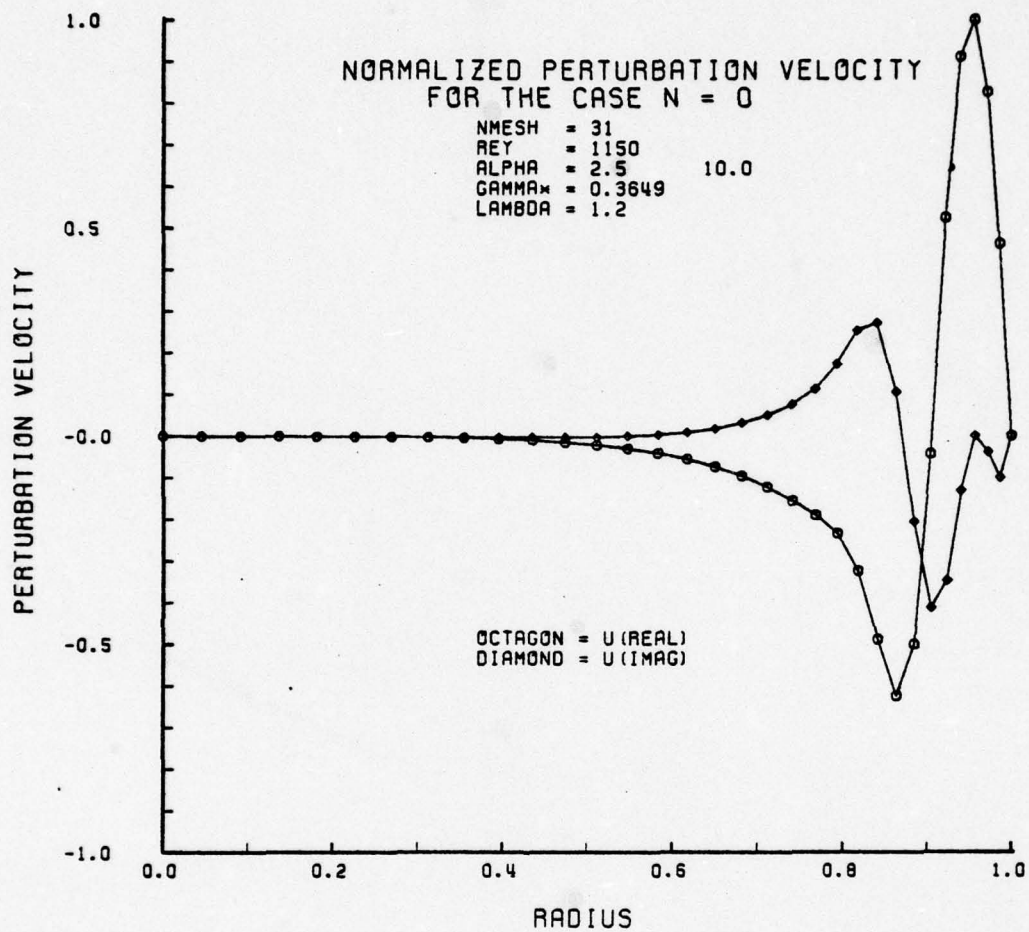


FIGURE 4-12

## V. CONCLUSIONS AND RECOMMENDATIONS

The implementation of the newly developed boundary conditions of Gawain [9] has permitted a stable, numerical solution to the linearized vorticity transport equation. The results of the numerical solution are presented in Section IV and show that the stability of pipe Poiseuille flow is governed by the three parameters,  $\alpha_R$ ,  $\alpha_I$  and  $R_e$ . In particular, both positive and negative values of  $\alpha_R$ , that is, streamwise growth and decay in space, if sufficiently large, produce unstable growth rates in time. This result is new and it is consistent with the known experimental fact that transition to turbulent flow depends not only on Reynolds number but also on the general character of the perturbations which exist in the flow.

The perturbation velocity plots of Section IV represent the first practical look at the function  $Q$ . These plots were valuable indicators for adequacy of mesh fineness, that is,  $N$ , changes in the nature of the function  $Q$  and effects of a nonuniform mesh.

No instabilities were discovered for purely sinusoidal perturbations ( $\alpha_R = 0$ ). This is consistent with the previous investigation of Ref. 11, but should not be assumed for investigations of other angular wave numbers, ( $n = 1, 2, 3, \dots$ ).



Adequate numerical accuracy was proven by demonstrating that the solution was virtually independent of the number of mesh points,  $N$ , and that it satisfied to a high degree an independent check of the governing differential equation. This procedure should also be carried out in future investigations prior to conducting full scale data runs.

This study suggests that similar, and perhaps even more rewarding results will be obtained for the higher angular wave numbers. Although lengthy, programming is straightforward if approached systematically. The general organization of the programs of Ref. 4 or Ref. 6 should be helpful in this task. It is recommended that the case for  $n = 1$  be undertaken as a follow-on to this study.

The nonuniform computational mesh was shown to be a powerful tool in the reduction of computational time. At the same time, however, the dependence of the mesh offset parameter,  $\lambda$ , on input conditions needs to be investigated further to realize the full potential of this technique.

## APPENDIX A

### DERIVATION OF VORTICITY TRANSPORT EQUATION COEFFICIENTS

From the change of variable introduced in Ref. 9, the function H for the case  $n = 0$  is expressed by

$$H = rQ \quad (A-1)$$

Taking derivatives

$$DH = rDQ + Q \quad (A-2)$$

$$D^2H = rD^2Q + 2DQ \quad (A-3)$$

$$D^3H = rD^3Q + 3D^2Q \quad (A-4)$$

$$D^4H = rD^4Q + 4D^3Q \quad (A-5)$$

Let the '\*' superscript denote element (2,2) of matrices (A1) through (A9) of Ref. 9. Since for  $n = 0$ , only the function H was investigated, equations (2-10) become

$$\begin{aligned} M_4^* D^4H + M_3^* D^3H + M_2^* D^2H + M_1^* DH + M_0^* H \\ - \gamma [N_2^* D^2H + N_1^* DH + N_0^* H] = 0 \end{aligned} \quad (A-6)$$

Substituting for H, equation (A-6) becomes

$$\begin{aligned}
& M_4^* \{rD^4Q + 4D^3Q\} + M_3^* \{rD^3Q + 3D^2Q\} + M_2^* \{rD^2Q + 2DQ\} \\
& + M_1^* \{rDQ + Q\} + M_0^* \{rQ\} - \gamma [N_2^* \{rD^2Q + 2DQ\} \\
& + N_1^* \{rDQ + Q\} + N_0^* \{rQ\}] = 0
\end{aligned} \tag{A-7}$$

Before proceeding further, it should be noted that the Ref. 9 matrices from which the coefficients for equation (A-7) were taken were obtained from matrices (2-10) through (2-17) of Ref. 6 by means of the following substitutions:

$$U = 2(1 - r^2) \tag{A-8}$$

$$t = \alpha^2 \frac{n_2}{r^2} \tag{A-9}$$

$$T = \alpha U - \frac{1}{R_e} \left( \alpha^2 - \frac{n_2}{r^2} \right) \tag{A-10}$$

Defining the new coefficients for equation (A-7) as  $M_0$  through  $M_4$  and  $N_0$  through  $N_2$

$$M_4 = rM_4^* = -\frac{r}{R_e} \tag{A-11}$$

$$M_3 = 4M_4^* + rM_3^* = -\frac{6}{R_e} \tag{A-12}$$

$$M_2 = 3M_3^* + rM_2^* = r\alpha U - \frac{1}{R_e} \left\{ \frac{3}{r} + 2\alpha^2 r \right\} \tag{A-13}$$

$$M_1 = 2M_2^* + rM_1^* = 3\alpha U + \frac{3}{R_e} \left\{ \frac{1}{r^2} - 2\alpha^2 \right\} \tag{A-14}$$

$$M_0 = M_1^* + rM_0^* = r\alpha^3 U - \frac{\alpha^4 r}{R_e} \tag{A-15}$$



$$N_2 = rN_2^* = -r \quad (A-16)$$

$$N_1 = 2N_2^* + rN_1^* = -3 \quad (A-17)$$

$$N_0 = N_1^* + rN_0^* = -\alpha^2 r \quad (A-18)$$

Upon making use of the foregoing substitutions, the governing relation can finally be reduced to the form previously shown in equation (3-1).

APPENDIX B  
FINITE DIFFERENCE EQUATIONS

Improved finite difference equations for the boundaries were obtained by not using the virtual point method of Ref. 4 and Ref. 6 and deriving the forms directly from the boundary conditions of Appendix A. The equations thus formed are also of consistent order truncation error, significantly improving the accuracy of the solution [Ref. 8].

Because of a peculiarity in the form of the consistent second order truncation error equations at the axis, a singularity resulted for  $\alpha$  equal to zero. Consistent third order truncation error equations eliminated this problem.

From Appendix A, the axis boundary conditions are

$$DQ(0) = 0 \quad \text{and} \quad D^3Q(0) = 0 \quad (B-1)$$

Representing  $Q$  by a power series and applying equations (B-1) yields

$$\begin{aligned} Q(r) = Q(0) + D^2Q(0)\frac{r^2}{2!} + D^4Q(0)\frac{r^4}{4!} + D^5Q(0)\frac{r^5}{5!} \\ + D^6Q(0)\frac{r^6}{6!} + \dots \end{aligned} \quad (B-2)$$

Using five mesh points at  $r = \delta, 2\delta, 3\delta, 4\delta$  and  $5\delta$  results in the matrix

$$\begin{bmatrix} Q_1 \\ Q_2 \\ Q_3 \\ Q_4 \\ Q_5 \end{bmatrix} = \begin{bmatrix} 1 & \frac{1}{2} & \frac{1}{24} & \frac{1}{120} & \frac{1}{720} \\ 1 & 2 & \frac{16}{24} & \frac{32}{120} & \frac{64}{720} \\ 1 & \frac{9}{2} & \frac{81}{24} & \frac{243}{120} & \frac{729}{720} \\ 1 & 8 & \frac{256}{24} & \frac{1024}{120} & \frac{4096}{720} \\ 1 & \frac{25}{2} & \frac{625}{24} & \frac{3125}{120} & \frac{15625}{720} \end{bmatrix} \begin{bmatrix} Q(0) \\ \delta^2 D^2 Q(0) \\ \delta^4 D^4 Q(0) \\ \delta^5 D^5 Q(0) \\ \delta^6 D^6 Q(0) \end{bmatrix} + O\delta^7$$

(B-3)

Differentiating equation (B-2) and substituting  $r = \delta$  gives  
(in matrix form)

$$\begin{bmatrix} Q(\delta) \\ \delta DQ(\delta) \\ \delta^2 D^2 Q(\delta) \\ \delta^3 D^3 Q(\delta) \\ \delta^4 D^4 Q(\delta) \end{bmatrix} = \begin{bmatrix} 1 & \frac{1}{2!} & \frac{1}{4!} & \frac{1}{5!} & \frac{1}{6!} \\ 0 & 1 & \frac{1}{3!} & \frac{1}{4!} & \frac{1}{5!} \\ 0 & 1 & \frac{1}{2!} & \frac{1}{3!} & \frac{1}{4!} \\ 0 & 0 & 1 & \frac{1}{2!} & \frac{1}{3!} \\ 0 & 0 & 1 & 1 & \frac{1}{2!} \end{bmatrix} \begin{bmatrix} Q(0) \\ \delta^2 D^2 Q(0) \\ \delta^4 D^4 Q(0) \\ \delta^5 D^5 Q(0) \\ \delta^6 D^6 Q(0) \end{bmatrix} + O\delta^7$$

(B-4)

Let [A] and [B] denote the coefficient matrices of equations (B-3) and (B-4) respectively. The values of  $Q(0)$ ,  $\delta^2 D^2 Q(0)$ ,  $\delta^4 D^4 Q(0)$ ,  $\delta^5 D^5 Q(0)$  and  $\delta^6 D^6 Q(0)$  may be solved for by



$$\begin{bmatrix} Q(0) \\ \delta^2 D^2 Q(0) \\ \delta^4 D^4 Q(0) \\ \delta^5 D^5 Q(0) \\ \delta^6 D^6 Q(0) \end{bmatrix} = [A]^{-1} \begin{bmatrix} Q_1 \\ Q_2 \\ Q_3 \\ Q_4 \\ Q_5 \end{bmatrix} + O\delta^7 \quad (B-5)$$

Putting equation (B-5) into equation (B-4),

$$\begin{bmatrix} Q(\delta) \\ \delta DQ(\delta) \\ \delta^2 D^2 Q(\delta) \\ \delta^3 D^3 Q(\delta) \\ \delta^4 D^4 Q(\delta) \end{bmatrix} = [B][A]^{-1} \begin{bmatrix} Q_1 \\ Q_2 \\ Q_3 \\ Q_4 \\ Q_5 \end{bmatrix} + O\delta^7 \quad (B-6)$$

The last line of this set of equations gives

$$\begin{aligned} D^4 Q(\delta) = & \frac{1}{\delta^4} (-0.911564626Q_1 + 2.750242955Q_2 - 3.043731779Q_3 \\ & + 1.42468416Q_4 - 0.219630709Q_5) + O\delta^3 \end{aligned} \quad (B-7)$$

To solve for  $D^3 Q(\delta)$ , the rightmost column and bottom row are eliminated from matrices [A] and [B] then these new matrices are inserted into equations (B-5) and (B-6).

The bottom line of equation (B-6) will now give the expression for  $D^3Q(\delta)$  with a consistent third order truncation error.  $D^2Q(\delta)$  and  $DQ(\delta)$  were solved for in a similar manner.

$$D^3Q(\delta) = \frac{1}{\delta^3}(1.825165563Q_1 - 3.250331126Q_2 + 1.660927152Q_3 - .235761589Q_4) + O\delta^3 \quad (B-8)$$

$$D^2Q = \frac{1}{\delta^2}(-\frac{35}{60}Q_1 + \frac{8}{15}Q_2 + \frac{1}{20}Q_3) + O\delta^3 \quad (B-9)$$

$$DQ = \frac{1}{\delta}(-\frac{2}{3}Q_1 + \frac{2}{3}Q_2) + O\delta^3 \quad (B-10)$$

Due to the complexity of the boundary conditions, it was decided that consistent third order truncation error equations should also be used at  $r = 2\delta$ . For this the [B] matrix only need be changed as equation (B-2) is unchanged at this station. The new matrix [B] is formed by differentiating equation (B-2) and making the substitution  $r = 2\delta$ . Proceeding as for  $r = \delta$  gives the following finite difference approximations

$$D^4Q(2\delta) = \frac{1}{\delta^4}(-3.10340136Q_1 + 6.903012634Q_2 - 5.342274053Q_3 + 1.66083577Q_4 - 0.123420797Q_5) + O\delta^3 \quad (B-11)$$

$$D^3Q(2\delta) = \frac{1}{\delta^3}(.868874172Q_1 - .937748345Q_2 - .254304636Q_3 + .323178808Q_4) + O\delta^3 \quad (B-12)$$

$$D^2 Q(2\delta) = \frac{1}{\delta^2} \left( \frac{11}{12} Q_1 - \frac{28}{15} Q_2 + \frac{19}{20} Q_3 \right) + O\delta^3 \quad (B-13)$$

$$DQ(2\delta) = \frac{1}{\delta} \left( -\frac{4}{3} Q_1 + \frac{4}{3} Q_2 \right) + O\delta^3 \quad (B-14)$$

It should also be noted that the value of  $Q$  at  $r = 0$  may be solved for from the top line of equations (B-5)

$$\begin{aligned} Q(0) = & (1.795918367Q_1 - 1.24781341Q_2 + .606413994Q_3 \\ & - .177842566Q_4 + .023323615Q_5) + O\delta^3 \end{aligned} \quad (B-15)$$

The central difference equations given by Ref. 6 were already consistent second order truncation error equations as confirmed by Ref. 8 and were retained.

For the wall, the clamped end, consistent second order equations (5) through (8) of Table II, Ref. 8 were modified for the "right boundary" using the procedure given in Section 5 of that reference.

$$D^4 Q(1-\delta) = \frac{1}{\delta^4} \left( -\frac{1}{4} Q_{N-3} + \frac{8}{3} Q_{N-2} - 9Q_{N-1} + 16Q_N \right) + O\delta^2 \quad (B-16)$$

$$D^3 Q(1-\delta) = \frac{1}{\delta^3} \left( -\frac{1}{3} Q_{N-2} + 3Q_N \right) + O\delta^2 \quad (B-17)$$

$$D^2 Q(1-\delta) = \frac{1}{\delta^2} (Q_{N-1} - 2Q_N) + O\delta^2 \quad (B-18)$$

$$DQ(1-\delta) = \frac{1}{\delta} \left( -\frac{1}{2} Q_{N-1} \right) + O\delta^2 \quad (B-19)$$



Since the wall finite difference approximations were of only second order truncation error, the approximations for  $DQ$  through  $D^4Q$  at  $r = 1-2\delta$  were obtained directly from the central difference equations with  $Q(1) = 0$ .

$$D^4Q(1-2\delta) = \frac{1}{\delta^4}(Q_{N-3} - 4Q_{N-2} + 6Q_{N-1} - 4Q_N) + O\delta^2 \quad (B-20)$$

$$D^3Q(1-2\delta) = \frac{1}{\delta^3}(-\frac{1}{2}Q_{N-3} + Q_{N-2} - Q_N) + O\delta^2 \quad (B-21)$$

$$D^2Q(1-2\delta) = \frac{1}{\delta^2}(Q_{N-2} - 2Q_{N-1} + Q_N) + O\delta^2 \quad (B-22)$$

$$DQ(1-2\delta) = \frac{1}{\delta}(-\frac{1}{2}Q_{N-2} + \frac{1}{2}Q_N) + O\delta^2 \quad (B-23)$$

## APPENDIX C

### NONUNIFORM MESH

To control the distribution of a fixed number of mesh points, a change of the independent variable from  $r$  to  $\eta$  was performed.

$$Q = Q(\eta) \quad (C-1)$$

$$r = r(\eta) \quad (C-2)$$

The derivative with respect to  $r$  becomes

$$D = (D^*r)^{-1}D^* \quad (C-3)$$

where

$$D^* = \frac{d}{d\eta} \quad \text{and} \quad D = \frac{d}{dr} \quad (C-4)$$

$DQ$ ,  $D^2Q$  ... can now be expressed in terms of the new independent variable,  $\eta$ .

$$DQ = (D^*r)^{-1}D^*Q \quad (C-5)$$

$$\begin{aligned} D^2Q &= D(DQ) = (D^*r)^{-1}D^*(DQ) \\ &= (D^*r)^{-2}D^{*2}Q - (D^*r)^{-3}(D^{*2}r)D^*Q \end{aligned} \quad (C-6)$$

$$\begin{aligned}
D^3 Q &= D(D^2 Q) = (D^* R)^{-1} D^* (D^2 Q) \\
&= (D^* r)^{-3} D^{*3} Q - 3(D^* r)^{-4} (D^{*2} r) D^{*2} Q \\
&\quad - [(D^* r)^{-4} (D^{*3} r) - 3(D^* r)^{-5} (D^{*2} r)^2] DQ \quad (C-7)
\end{aligned}$$

$$\begin{aligned}
D^4 Q &= D(D^3 Q) = (D^* r)^{-1} D^* (D^3 Q) \\
&= (D^* r)^{-4} D^{*4} Q - 6(D^* r)^{-5} (D^{*2} r) D^{*3} Q \\
&\quad + [15(D^* r)^{-6} (D^{*2} r) - 4(D^* r)^{-5} (D^{*3} r)] D^{*2} Q \\
&\quad - [15(D^* r)^{-7} (D^{*2} r)^3 - 10(D^* r)^{-6} (D^{*2} r) (D^{*3} r) \\
&\quad + (D^* r)^{-5} (D^{*4} r)] DQ \quad (C-8)
\end{aligned}$$

The derivatives of  $Q$  with respect to  $r$  can now be written

$$DQ = f_{11} D^* Q \quad (C-9)$$

$$D^2 Q = f_{22} D^{*2} Q + f_{21} D^* Q \quad (C-10)$$

$$D^3 Q = f_{33} D^{*3} Q + f_{32} D^{*2} Q + f_{31} D^* Q \quad (C-11)$$

$$D^4 Q = f_{44} D^{*4} Q + f_{43} D^{*3} Q + f_{42} D^{*2} Q + f_{41} D^* Q \quad (C-12)$$

where

$$f_{11} = (D^* r)^{-1} \quad (C-13)$$



$$f_{22} = (D^* r)^{-2} \quad (C-14)$$

$$f_{21} = -(D^* r)^{-3} (D^{*2} r) \quad (C-15)$$

$$f_{33} = (D^* r)^{-3} \quad (C-16)$$

$$f_{32} = -3(D^* r)^{-4} (D^{*2} r) \quad (C-17)$$

$$f_{31} = 3(D^* r)^{-5} (D^{*2} r)^2 - (D^* r)^{-4} (D^{*3} r) \quad (C-18)$$

$$f_{44} = (D^* r)^{-4} \quad (C-19)$$

$$f_{43} = -6(D^* r)^{-5} (D^{*2} r) \quad (C-20)$$

$$f_{42} = 15(D^* r)^{-6} (D^{*2} r)^2 - 4(D^* r)^{-5} (D^{*3} r) \quad (C-21)$$

$$f_{41} = -15(D^* r)^{-7} (D^{*2} r)^3 + 10(D^* r)^{-6} (D^{*2} r) (D^{*3} r) \\ - (D^* r)^{-5} (D^{*4} r) \quad (C-22)$$

Substituting equations (C-9) through (C-12) into the vorticity transport equation (A-6) yields

$$M_4^* D^{*4} Q + M_3^* D^{*3} Q + M_2^* D^{*2} Q + M_1^* D^* Q + M_0^* Q \\ - \gamma [N_2^* D^{*2} Q + N_1^* D^* Q + N_0^* Q] = 0 \quad (C-23)$$

where

$$M_4^* = M_4 f_{44} \quad (C-24)$$

$$M_3^* = M_4 f_{43} + M_3 f_{33} \quad (C-25)$$

$$M_2^* = M_4 f_{42} + M_3 f_{32} + M_2 f_{22} \quad (C-26)$$

$$M_1^* = M_4 f_{41} + M_3 f_{31} + M_2 f_{21} \quad (C-27)$$

$$M_0^* = M_0 \quad (C-28)$$

$$N_2^* = N_2 f_{22} \quad (C-29)$$

$$N_1^* = N_2 f_{21} + N_1 f_{11} \quad (C-30)$$

$$N_0^* = N \quad (C-31)$$

In order to concentrate the mesh points at the axis, the function

$$r = 1 - C \tanh \lambda(1-\eta) \quad (C-32)$$

was chosen where  $\lambda$  is a parameter controlling the degree of concentration of mesh points near the axis. Equation (C-32) must satisfy the two conditions

$$r = 0 \quad \text{at} \quad \eta = 0 \quad (C-33)$$

and

$$r = 1 \quad \text{at} \quad \eta = 1 .$$

Substituting equation (C-33) into (C-32) gives

$$C = 1/\tanh \lambda . \quad (C-35)$$

Computing derivatives

$$D^*_r = C\lambda/\cosh^2\lambda(1-\eta) \quad (C-36)$$

$$D^{*2}_r = 2C\lambda^2[\tanh\lambda(1-\eta)/\cosh^2\lambda(1-\eta)] \quad (C-37)$$

$$D^{*3}_r = -2C\lambda^3\{[1-2\sinh^2\lambda(1-\eta)]/\cosh^4\lambda(1-\eta)\} \quad (C-38)$$

$$D^{*4}_r = 8C\lambda^4[\tanh^3\lambda(1-\eta)/\cosh^2\lambda(1-\eta)] \quad (C-39)$$

To shift the mesh point concentration to the wall, the function

$$r = C \tanh \lambda \eta \quad (C-40)$$

was selected. Satisfying equations (C-33) and (C-34) for this equation also gives equation (C-35). The derivatives



of (C-40) are given by equations (C-36) through (C-39) if  $\eta$  is substituted for all occurrences of  $(1-\eta)$  and the signs of equations (C-37) and (C-39) are reversed. Figures C-1 and C-2 show equations (C-32) and (C-40) for four selected values of the parameter  $\lambda$ .

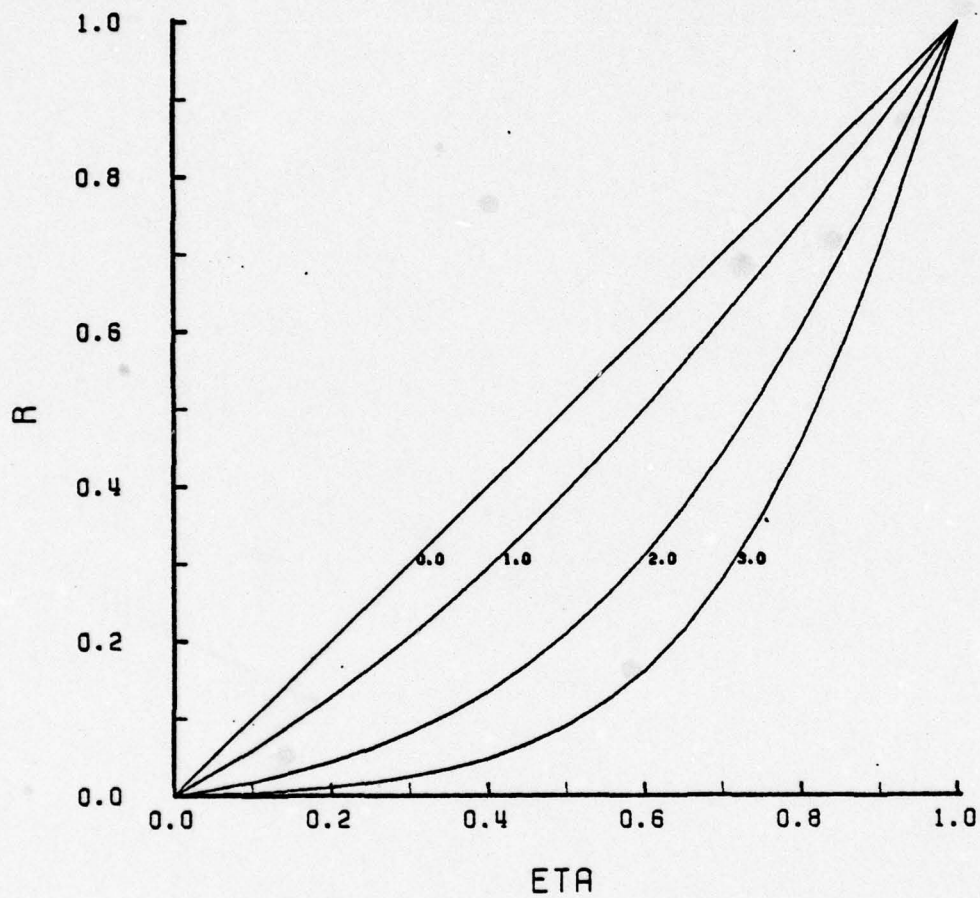


FIGURE C-1.  $R$  Versus  $\eta$  for Four Selected Values of  $\lambda$  - Axis Offset

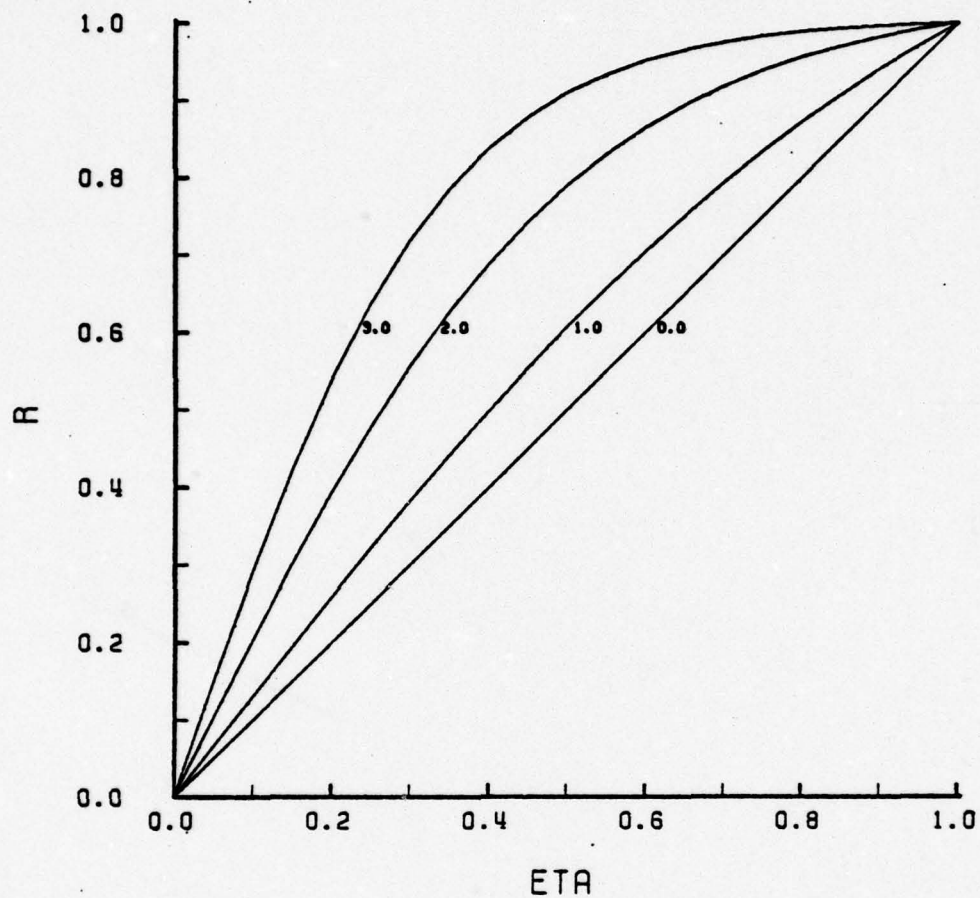


FIGURE C-2.  $R$  Versus  $\eta$  for Four Selected Values of  $\lambda$  - Wall Offset



# APPENDIX D

## DERIVATION OF PERTURBATION VELOCITIES

From Ref. 4, Appendix E, equations E-6 through E-8:

$$\begin{bmatrix} u(r) \\ v(r) \\ w(r) \end{bmatrix} = [A]\bar{W} + [B]D\bar{W} \quad (D-1)$$

$$= \begin{bmatrix} 0 & -\frac{\beta}{r} & \frac{1}{r} \\ \frac{\beta}{r} & 0 & -\alpha \\ 0 & \alpha & 0 \end{bmatrix} \begin{bmatrix} F \\ G \\ H \end{bmatrix} + \begin{bmatrix} 0 & 0 & 1 \\ 0 & 0 & 0 \\ -1 & 0 & 0 \end{bmatrix} \begin{bmatrix} DF \\ DG \\ DG \end{bmatrix} \quad (D-2)$$

For this case  $\beta = \eta_i = 0$  and  $F = DF = 0$ . Restricting the investigation to the function  $H$  for the reason expressed in Section I and solving for  $u(r)$  gives

$$u(r) = \frac{H}{r} + DH \quad (D-3)$$

Performing the change of variable

$$H = rQ \quad (D-4)$$

$$DH = Q + rDQ \quad (D-5)$$

$$u(r) = \frac{rQ}{r} + (Q + rDQ) = 2Q + rDQ \quad (D-6)$$

In order to implement this derivation in a numerical analysis, equation (D-6) was rewritten as

$$u_i = 2Q_i + r_i DQ_i \quad (D-7)$$

Performing the change of independent variable (Appendix C) to accommodate a nonuniform mesh

$$Q_i = Q(\eta_i) \quad (D-8)$$

$$r_i = r(\eta_i) \quad (D-9)$$

$$DQ_i = (D^* r_i)^{-1} D^* Q(\eta_i) \quad (D-10)$$

Substituting equations (D-8), (D-9) and (D-10) into equation (D-7) gives

$$u_i = 2Q(\eta_i) + r(\eta_i) (D^* r_i)^{-1} D^* Q(\eta_i) \quad (D-11)$$

For the axis offset nonuniform mesh,  $r(\eta)$  is given by equation (C-32) and  $(D^* r)$  by equation (C-36). Substituting into equation (D-11) using equation (C-35) results in

$$\begin{aligned}
u_i &= 2Q(\eta_i) + \left\{ 1 - \frac{\tanh[\lambda(1-\eta_i)]}{\tanh \lambda} \right\} \left\{ \frac{\cosh^2[\lambda(1-\eta_i)]}{C\lambda} \right\} D^* Q(\eta_i) \\
&= 2Q(\eta_i) + \left\{ 1 - \frac{\tanh[\lambda(1-\eta_i)]}{\tanh \lambda} \right\} \frac{\tanh \lambda \cosh^2[\lambda(1-\eta_i)]}{\lambda} \left\{ D^* Q(\eta_i) \right\}
\end{aligned}
\tag{D-12}$$

For the wall offset mesh, equation (C-40) is substituted for equation (C-32) and all occurrences of the term  $1-\eta_i$  are replaced by the term  $\eta_i$ .

The value of  $u$  at the axis ( $u_0$ ) and at the wall ( $u_{N+1}$ ) were solved for by using the boundary conditions specified in Ref. 9, namely

$$Q(1) = 0 \tag{D-13}$$

$$DQ(1) = 0 \tag{D-14}$$

$$DQ(0) = 0 \tag{D-15}$$

$$D^3Q(0) = 0 \tag{D-16}$$

From equations (D-13) and (D-14), using equation (D-7) it is obvious that

$$u_{N+1} = 0 \tag{D-17}$$

and from equations (D-15) and (D-7), it is similarly found that



$$u_0 = 2Q(0) ,$$

(D-18)

where the finite difference approximation for  $Q(0)$  is given by equation (B-15).











```

290      MODENO - AN INTEGER CONTROLLING THE OUTPUT OF
300      OF EIGENVECTORS TO FILE FT02F001. IF MODENO
310      IS EQUAL TO +1, EIGENVECTORS ARE OUTPUT;
320      OTHERWISE OUTPUT IS INHIBITED.
330
340      OTHER ROUTINES NEEDED
350
360      MSET2,CDMTIN,MULM,DSPLIT,EHESSC,ELRH2C,EEALAC,EBBCKC
370
380      .....
390
400      SUBROUTINE STAB (AR,AI,GRMAX,KSET,MODENO)
410      IMPLICIT REAL*8(A-H,O-Z)
420      COMPLEX *16A,G
430      COMPLEX *16CQM1E1,CQM2E1
440
450      NOTE---CHANGE DIMENSIONS FROM HERE THROUGH 'N' = 1 FOR
460      NEW NMESH. CP/CMS MAX NMESH IS 79. LOGIN WITH 520K OF CORE.
470
480      REAL *8GR(79),GI(79),ZR(79,79),ZI(79,79),RADIUS(79),CVEC(79)
490      COMPLEX *16XMAT(79,79),YMAT(79,79),WV(79)
500      DIMENSION IVEC(79)
510      COMMON /COEFNT/ A,G,REY,DELR,AMDA
520      EXTERNAL CQM1E1,CQM2E1
530
540      A = DCMLPX(AR,AI)
550      MDIM = 79
560      N = 79
570
580      SET UP THE CENTRAL DIFFERENCE APPROXIMATION AT EACH POINT IN
590      THE MESH FOR THOSE TERMS IN THE VORTICITY TRANSPORT EQUATION
600      WHICH DO NOT CONTAIN GAMMA AS A FACTOR.
610
620      CALL MSET2 (XMAT,N,MDIM,CQM1E1,KSET)
630
640      SET UP THE CENTRAL DIFFERENCE APPROXIMATION AT EACH POINT IN
650      THE MESH FOR THOSE TERMS IN THE VORTICITY TRANSPORT EQUATION
660      WHICH CONTAIN GAMMA AS A FACTOR.
670
680      CALL MSET2 (YMAT,N,MDIM,CQM2E1,KSET)
690
700
710
720
730
740
750
760

```























```

123D0*CQM1(3)/(15D0*DEL**2)+4D0*CQM1(2)/(3D0*DEL)+CQM1(1)
GO TO 29
10 CQM1E1 = -5.342274053D0*CQM1(5)/DEL**4-.254204636D0*CQM1(4)/DEL**3
1+19D0*CQM1(3)/(20D0*DEL**2)
GO TO 29
11 CQM1E1 = 1.666083577D0*CQM1(5)/DEL**4+.3231788C8D C*CQM1(4)/DEL**3
GO TO 29
12 CQM1E1 = -0.123420797D0*CQM1(5)/DEL**4
GO TO 29

      CENTRAL DIFFERENCE APPROXIMATION FOR COMPONENT Q (NON GAMMA).

13 GO TO (14,15,16,17,18), K
14 CQM1E1 = CQM1(5)/DEL**4-CQM1(4)/(2D0*DEL**3)
GO TO 29
15 CQM1E1 = -4D0*CQM1(5)/DEL**4+CQM1(4)/DEL**3+CQM1(3)/DEL**2-CQM1(2)
1/(2D0*DEL)
GO TO 29
16 CQM1E1 = 6D0*CQM1(5)/DEL**4-2D0*CQM1(3)/DEL**2+CQM1(1)
GO TO 29
17 CQM1E1 = -4D0*CQM1(5)/DEL**4-CQM1(4)/DEL**3+CQM1(3)/DEL**2+CQM1(2)
1/(2D0*DEL)
GO TO 29
18 CQM1E1 = CQM1(5)/DEL**4+CQM1(4)/(2D0*DEL**3)
GO TO 29

      FINITE DIFFERENCE EQUATIONS AT ETA=1D0-2D0*DEL (NCN-GAMMA).

19 GO TO (20,21,22,23), K
20 CQM1E1 = CQM1(5)/DEL**4-0.5D0*CQM1(4)/DEL**3
GO TO 29
21 CQM1E1 = -4D0*CQM1(5)/DEL**4+CQM1(4)/DEL**3+CQM1(3)/DEL**2-CQM1(2)
1/(2D0*DEL)
GO TO 29
22 CQM1E1 = 6D0*CQM1(5)/DEL**4-2D0*CQM1(3)/DEL**2+CQM1(1)
GO TO 29
23 CQM1E1 = -4D0*CQM1(5)/DEL**4-CQM1(4)/DEL**3+CQM1(3)/DEL**2+CQM1(2)
1/(2D0*DEL)
GO TO 29

      FINITE DIFFERENCE EQUATIONS AT ETA=1D0-DEL (NON GAMMA).

24 GO TO (25,26,27,28), K
25 CQM1E1 = -0.25D0*CQM1(5)/DEL**4
GO TO 29
26 CQM1E1 = 8D0*CQM1(5)/(3D0*DEL**4)-CQM1(4)/(3D0*DEL**3)
GO TO 29
27 CQM1E1 = -9D0*CQM1(5)/DEL**4+CQM1(3)/DEL**2-CQM1(2)/(2D0*DEL)
GO TO 29

```

CQM1 930  
 CQM1 940  
 CQM1 950  
 CQM1 960  
 CQM1 970  
 CQM1 980  
 CQM1 990  
 CQM1 1000  
 CQM1 1010  
 CQM1 1020  
 CQM1 1030  
 CQM1 1040  
 CQM1 1050  
 CQM1 1060  
 CQM1 1070  
 CQM1 1080  
 CQM1 1090  
 CQM1 1100  
 CQM1 1110  
 CQM1 1120  
 CQM1 1130  
 CQM1 1140  
 CQM1 1150  
 CQM1 1160  
 CQM1 1170  
 CQM1 1180  
 CQM1 1190  
 CQM1 1200  
 CQM1 1210  
 CQM1 1220  
 CQM1 1230  
 CQM1 1240  
 CQM1 1250  
 CQM1 1260  
 CQM1 1270  
 CQM1 1280  
 CQM1 1290  
 CQM1 1300  
 CQM1 1310  
 CQM1 1320  
 CQM1 1330  
 CQM1 1340  
 CQM1 1350  
 CQM1 1360  
 CQM1 1370  
 CQM1 1380  
 CQM1 1390  
 CQM1 1400



```

GO TO 29
28 CQM1E1 = 16D0*CQM1(5)/DEL**4+3D0*CQM1(4)/DEL**3-2D0*CQM1(3)/DEL**2
29 RETURN
C
ENTRY CQM2E1(JSTA,K,CQM1,CQM2)
C
GO TO (30,35,40,45,5C), JSTA
C
FINITE DIFFERENCE EQUATIONS AT ETA=DEL (GAMMA).
C
GO TO (31,32,33,34,34), K
30 CQM2E1 = -35D0*CQM2(3)/(60D0*DEL**2)-2D0*CQM2(2)/(3D0*DEL)+CQM2(1)
31 GO TO 54
32 CQM2E1 = 8D0*CQM2(3)/(15D0*DEL**2)+2D0*CQM2(2)/(3D0*DEL)
33 GO TO 54
34 CQM2E1 = CQM2(3)/(20D0*DEL**2)
35 GO TO 54
36 CQM2E1 = (0D0,0D0)
C
FINITE DIFFERENCE EQUATIONS AT ETA=2D0*DEL (GAMMA)
C
GO TO (36,37,38,39,39), K
35 CQM2E1 = 11D0*CQM2(3)/(12D0*DEL**2)-4D0*CQM2(2)/(3D0*DEL)
36 GO TO 54
37 CQM2E1 = -28D0*CQM2(3)/(15D0*DEL**2)+4D0*CQM2(2)/(3D0*DEL)+CQM2(1)
38 GO TO 54
39 CQM2E1 = 19D0*CQM2(3)/(20D0*DEL**2)
40 GO TO 54
41 CQM2E1 = (0D0,0D0)
C
CENTRAL DIFFERENCE EQUATIONS FOR THE COMPONENT Q (GAMMA).
C
GO TO (41,42,43,44,41), K
40 CQM2E1 = (0D0,0D0)
41 GO TO 54
42 CQM2E1 = CQM2(3)/DEL**2-CQM2(2)/(2D0*DEL)
43 GO TO 54
44 CQM2E1 = -2D0*CQM2(3)/DEL**2+CQM2(1)
45 GO TO 54
46 CQM2E1 = CQM2(3)/DEL**2+CQM2(2)/(2D0*DEL)
47 GO TO 54
48 CQM2E1 = CQM2(3)/DEL**2+CQM2(2)/(2D0*DEL)
49 GO TO 54
50 CQM2E1 = CQM2(3)/DEL**2+CQM2(2)/(2D0*DEL)
51 GO TO 54
52 CQM2E1 = CQM2(3)/DEL**2+CQM2(2)/(2D0*DEL)
53 GO TO 54
54 CQM2E1 = CQM2(3)/DEL**2+CQM2(2)/(2D0*DEL)
55 GO TO 54
56 CQM2E1 = CQM2(3)/DEL**2+CQM2(2)/(2D0*DEL)
57 GO TO 54
58 CQM2E1 = CQM2(3)/DEL**2+CQM2(2)/(2D0*DEL)
59 GO TO 54
60 CQM2E1 = CQM2(3)/DEL**2+CQM2(2)/(2D0*DEL)
61 GO TO 54
62 CQM2E1 = CQM2(3)/DEL**2+CQM2(2)/(2D0*DEL)
63 GO TO 54
64 CQM2E1 = CQM2(3)/DEL**2+CQM2(2)/(2D0*DEL)
65 GO TO 54
66 CQM2E1 = CQM2(3)/DEL**2+CQM2(2)/(2D0*DEL)
67 GO TO 54
68 CQM2E1 = CQM2(3)/DEL**2+CQM2(2)/(2D0*DEL)
69 GO TO 54
70 CQM2E1 = CQM2(3)/DEL**2+CQM2(2)/(2D0*DEL)
71 GO TO 54
72 CQM2E1 = CQM2(3)/DEL**2+CQM2(2)/(2D0*DEL)
73 GO TO 54
74 CQM2E1 = CQM2(3)/DEL**2+CQM2(2)/(2D0*DEL)
75 GO TO 54
76 CQM2E1 = CQM2(3)/DEL**2+CQM2(2)/(2D0*DEL)
77 GO TO 54
78 CQM2E1 = CQM2(3)/DEL**2+CQM2(2)/(2D0*DEL)
79 GO TO 54
80 CQM2E1 = CQM2(3)/DEL**2+CQM2(2)/(2D0*DEL)
81 GO TO 54
82 CQM2E1 = CQM2(3)/DEL**2+CQM2(2)/(2D0*DEL)
83 GO TO 54
84 CQM2E1 = CQM2(3)/DEL**2+CQM2(2)/(2D0*DEL)
85 GO TO 54
86 CQM2E1 = CQM2(3)/DEL**2+CQM2(2)/(2D0*DEL)
87 GO TO 54
88 CQM2E1 = CQM2(3)/DEL**2+CQM2(2)/(2D0*DEL)
89 GO TO 54
90 CQM2E1 = CQM2(3)/DEL**2+CQM2(2)/(2D0*DEL)
91 GO TO 54
92 CQM2E1 = CQM2(3)/DEL**2+CQM2(2)/(2D0*DEL)
93 GO TO 54
94 CQM2E1 = CQM2(3)/DEL**2+CQM2(2)/(2D0*DEL)
95 GO TO 54
96 CQM2E1 = CQM2(3)/DEL**2+CQM2(2)/(2D0*DEL)
97 GO TO 54
98 CQM2E1 = CQM2(3)/DEL**2+CQM2(2)/(2D0*DEL)
99 GO TO 54
100 CQM2E1 = CQM2(3)/DEL**2+CQM2(2)/(2D0*DEL)
101 GO TO 54
102 CQM2E1 = CQM2(3)/DEL**2+CQM2(2)/(2D0*DEL)
103 GO TO 54
104 CQM2E1 = CQM2(3)/DEL**2+CQM2(2)/(2D0*DEL)
105 GO TO 54
106 CQM2E1 = CQM2(3)/DEL**2+CQM2(2)/(2D0*DEL)
107 GO TO 54
108 CQM2E1 = CQM2(3)/DEL**2+CQM2(2)/(2D0*DEL)
109 GO TO 54
110 CQM2E1 = CQM2(3)/DEL**2+CQM2(2)/(2D0*DEL)
111 GO TO 54
112 CQM2E1 = CQM2(3)/DEL**2+CQM2(2)/(2D0*DEL)
113 GO TO 54
114 CQM2E1 = CQM2(3)/DEL**2+CQM2(2)/(2D0*DEL)
115 GO TO 54
116 CQM2E1 = CQM2(3)/DEL**2+CQM2(2)/(2D0*DEL)
117 GO TO 54
118 CQM2E1 = CQM2(3)/DEL**2+CQM2(2)/(2D0*DEL)
119 GO TO 54
120 CQM2E1 = CQM2(3)/DEL**2+CQM2(2)/(2D0*DEL)
121 GO TO 54
122 CQM2E1 = CQM2(3)/DEL**2+CQM2(2)/(2D0*DEL)
123 GO TO 54
124 CQM2E1 = CQM2(3)/DEL**2+CQM2(2)/(2D0*DEL)
125 GO TO 54
126 CQM2E1 = CQM2(3)/DEL**2+CQM2(2)/(2D0*DEL)
127 GO TO 54
128 CQM2E1 = CQM2(3)/DEL**2+CQM2(2)/(2D0*DEL)
129 GO TO 54
130 CQM2E1 = CQM2(3)/DEL**2+CQM2(2)/(2D0*DEL)
131 GO TO 54
132 CQM2E1 = CQM2(3)/DEL**2+CQM2(2)/(2D0*DEL)
133 GO TO 54
134 CQM2E1 = CQM2(3)/DEL**2+CQM2(2)/(2D0*DEL)
135 GO TO 54
136 CQM2E1 = CQM2(3)/DEL**2+CQM2(2)/(2D0*DEL)
137 GO TO 54
138 CQM2E1 = CQM2(3)/DEL**2+CQM2(2)/(2D0*DEL)
139 GO TO 54
140 CQM2E1 = CQM2(3)/DEL**2+CQM2(2)/(2D0*DEL)
141 GO TO 54
142 CQM2E1 = CQM2(3)/DEL**2+CQM2(2)/(2D0*DEL)
143 GO TO 54
144 CQM2E1 = CQM2(3)/DEL**2+CQM2(2)/(2D0*DEL)
145 GO TO 54
146 CQM2E1 = CQM2(3)/DEL**2+CQM2(2)/(2D0*DEL)
147 GO TO 54
148 CQM2E1 = CQM2(3)/DEL**2+CQM2(2)/(2D0*DEL)
149 GO TO 54
150 CQM2E1 = CQM2(3)/DEL**2+CQM2(2)/(2D0*DEL)
151 GO TO 54
152 CQM2E1 = CQM2(3)/DEL**2+CQM2(2)/(2D0*DEL)
153 GO TO 54
154 CQM2E1 = CQM2(3)/DEL**2+CQM2(2)/(2D0*DEL)
155 GO TO 54
156 CQM2E1 = CQM2(3)/DEL**2+CQM2(2)/(2D0*DEL)
157 GO TO 54
158 CQM2E1 = CQM2(3)/DEL**2+CQM2(2)/(2D0*DEL)
159 GO TO 54
160 CQM2E1 = CQM2(3)/DEL**2+CQM2(2)/(2D0*DEL)
161 GO TO 54
162 CQM2E1 = CQM2(3)/DEL**2+CQM2(2)/(2D0*DEL)
163 GO TO 54
164 CQM2E1 = CQM2(3)/DEL**2+CQM2(2)/(2D0*DEL)
165 GO TO 54
166 CQM2E1 = CQM2(3)/DEL**2+CQM2(2)/(2D0*DEL)
167 GO TO 54
168 CQM2E1 = CQM2(3)/DEL**2+CQM2(2)/(2D0*DEL)
169 GO TO 54
170 CQM2E1 = CQM2(3)/DEL**2+CQM2(2)/(2D0*DEL)
171 GO TO 54
172 CQM2E1 = CQM2(3)/DEL**2+CQM2(2)/(2D0*DEL)
173 GO TO 54
174 CQM2E1 = CQM2(3)/DEL**2+CQM2(2)/(2D0*DEL)
175 GO TO 54
176 CQM2E1 = CQM2(3)/DEL**2+CQM2(2)/(2D0*DEL)
177 GO TO 54
178 CQM2E1 = CQM2(3)/DEL**2+CQM2(2)/(2D0*DEL)
179 GO TO 54
180 CQM2E1 = CQM2(3)/DEL**2+CQM2(2)/(2D0*DEL)
181 GO TO 54
182 CQM2E1 = CQM2(3)/DEL**2+CQM2(2)/(2D0*DEL)
183 GO TO 54
184 CQM2E1 = CQM2(3)/DEL**2+CQM2(2)/(2D0*DEL)
185 GO TO 54
186 CQM2E1 = CQM2(3)/DEL**2+CQM2(2)/(2D0*DEL)
187 GO TO 54
188 CQM2E1 = CQM2(3)/DEL**2+CQM2(2)/(2D0*DEL)
189 GO TO 54
190 CQM2E1 = CQM2(3)/DEL**2+CQM2(2)/(2D0*DEL)
191 GO TO 54
192 CQM2E1 = CQM2(3)/DEL**2+CQM2(2)/(2D0*DEL)
193 GO TO 54
194 CQM2E1 = CQM2(3)/DEL**2+CQM2(2)/(2D0*DEL)
195 GO TO 54
196 CQM2E1 = CQM2(3)/DEL**2+CQM2(2)/(2D0*DEL)
197 GO TO 54
198 CQM2E1 = CQM2(3)/DEL**2+CQM2(2)/(2D0*DEL)
199 GO TO 54
200 CQM2E1 = CQM2(3)/DEL**2+CQM2(2)/(2D0*DEL)
201 GO TO 54
202 CQM2E1 = CQM2(3)/DEL**2+CQM2(2)/(2D0*DEL)
203 GO TO 54
204 CQM2E1 = CQM2(3)/DEL**2+CQM2(2)/(2D0*DEL)
205 GO TO 54
206 CQM2E1 = CQM2(3)/DEL**2+CQM2(2)/(2D0*DEL)
207 GO TO 54
208 CQM2E1 = CQM2(3)/DEL**2+CQM2(2)/(2D0*DEL)
209 GO TO 54
210 CQM2E1 = CQM2(3)/DEL**2+CQM2(2)/(2D0*DEL)
211 GO TO 54
212 CQM2E1 = CQM2(3)/DEL**2+CQM2(2)/(2D0*DEL)
213 GO TO 54
214 CQM2E1 = CQM2(3)/DEL**2+CQM2(2)/(2D0*DEL)
215 GO TO 54
216 CQM2E1 = CQM2(3)/DEL**2+CQM2(2)/(2D0*DEL)
217 GO TO 54
218 CQM2E1 = CQM2(3)/DEL**2+CQM2(2)/(2D0*DEL)
219 GO TO 54
220 CQM2E1 = CQM2(3)/DEL**2+CQM
```

COM11890  
COM11900  
COM11910  
COM11920  
COM11930  
COM11940  
COM11950  
COM11960  
COM11970  
COM11980  
COM11990  
COM12000  
COM12010  
COM12020  
COM12030  
COM12040  
COM12050  
COM12060

```

6C TO 54      -200*COM2(3)/DEL**2+COM2(1)
47 COM2E1 =
6C TO 54      COM2(3)/DEL**2+COM2(2)/(200*DEL)
48 COM2E1 =
6C TO 54      (000,000)
49 COM2E1 =
6C TO 54

      FINITE DIFFERENCE EQUATIONS AT ETA=100-DEL (GAMMA).
50 GO TO (53,52,51,52), K
51 COM2E1 = COM2(3)/DEL**2-COM2(2)/(200*DEL)
52 COM2E1 = -200*COM2(3)/DEL**2+COM2(1)
53 COM2E1 = (000,000)
54 RETURN
END

```

CC

CDMT 10  
CDMT 20  
CDMT 30  
CDMT 40  
CDMT 50  
CDMT 60  
CDMT 70  
CDMT 80  
CDMT 90  
CDMT 100  
CDMT 110  
CDMT 120  
CDMT 130  
CDMT 140  
CDMT 150  
CDMT 160  
CDMT 170  
CDMT 180  
CDMT 190  
CDMT 200  
CDMT 210  
CDMT 220  
CDMT 230  
CDMT 240  
CDMT 250  
CDMT 260  
CDMT 270  
CDMT 280

```

.....SUBROUTINE CDMTIN(N,A,NDIM,IERR).....
PURPOSE
      INVERT A COMPLEX*16 MATRIX
USAGE
      CALL CDMTIN(N,A,NDIM,DETERM)
DESCRIPTION OF PARAMETERS
      N      - ORDER OF COMPLEX*16 MATRIX TO BE INVERTED
              (INTEGER) MAXIMUM 'N' IS 100
      A      - COMPLEX*16 INPUT MATRIX (DESTROYED). THE
              INVERSE OF 'A' IS RETURNED IN ITS PLACE
      NDIM   - THE SIZE TO WHICH 'A' IS DIMENSIONED
              (ROW DIMENSION OF 'A' ACTUALLY APPEARING
              IN THE DIMENSION STATEMENT OF USER'S
              CALLING PROGRAM)
      IERR   - ERROR PARAMETER RETURNED BY CDMTIN. IERR = 0 INDICATES
              NORMAL INVERSION. IERR = 9999 INDICATES SINGULAR MATRIX.
REMARKS

```

CCCCCCCCCCCCCCCCCCCCCCCCCCCCCCCCCCCC





CDMT 770  
CDMT 780  
CDMT 790  
CDMT 800  
CDMT 810  
CDMT 820  
CDMT 830  
CDMT 840  
CDMT 850  
CDMT 860  
CDMT 870  
CDMT 880  
CDMT 890  
CDMT 900  
CDMT 910  
CDMT 920  
CDMT 930  
CDMT 940  
CDMT 950  
CDMT 960  
CDMT 970  
CDMT 980  
CDMT 990  
CDMT 1000  
CDMT 1010  
CDMT 1020  
CDMT 1030  
CDMT 1040  
CDMT 1050  
CDMT 1060  
CDMT 1070  
CDMT 1080  
CDMT 1090  
CDMT 1100  
CDMT 1110  
CDMT 1120  
CDMT 1130  
CDMT 1140  
CDMT 1150  
CDMT 1160  
CDMT 1170  
CDMT 1180  
CDMT 1190  
CDMT 1200  
CDMT 1210  
CDMT 1220  
CDMT 1230  
CDMT 1240

```

ICOLUM = K
AMAX = A(J,K)
6 CONTINUE
7 CCNTINUE
  IPIVOT(ICOLUM) = IPIVOT(ICOLUM)+1
  INTERCHANGE ROWS TO PUT PIVOT ELEMENT ON DIAGONAL
  IF (IROW-ICOLUM) 8,10,8
8 CONTINUE
  DC 9 L=1,N
  SWAP = A(IROW,L)
  A(IROW,L) = A(ICOLUM,L)
  A(ICOLUM,L) = SWAP
9
  SWAP = ALPHA(IROW)
  ALPHA(IROW) = ALPHA(ICOLUM)
  ALPHA(ICOLUM) = SWAP
10 INDEX(I,1) = IROW
  INDEX(I,2) = ICOLUM
  PIVOT(I) = A(ICOLUM, ICOLUM)
  U = PIVOT(I)
  TEMP = PIVOT(I)*DCONJG(PIVOT(I))
  IF (TEMP) 11,20,11
    DIVIDE PIVOT ROW BY PIVOT ELEMENT
11 A(ICOLUM,ICOLUM) = (1CO,ODO)
  DC 12 L=1,N
  U = PIVOT(I)
12 A(ICOLUM,L) = A(ICOLUM,L)/U
    REDUCE NON-PIVOT ROWS
  CO 15 L=1,N
  IF (L1-ICOLUM) 13,15,13
13 T = A(L1,ICOLUM)
  A(L1,ICOLUM) = (OCO,ODO)
  CO 14 L=1,N
  U = A(ICOLUM,L)
14 A(L1,L) = A(L1,L)-U*T

```



```

X2 - THE MULTIPLIED MATRIX.
N - THE ORDER OF X1 AND X2.
MDIM - THE DIMENSION OF X1 AND X2 FROM THE CALLING PROGRAM.
TEMPV - A WORKING VECTOR. MUST BE DIMENSIONED MDIM.
OTHER ROUTINES REQUIRED
NONE
.....
SUBROUTINE MULM (X1,X2,N,MDIM,TEMPV)
  COMPLEX *16 X1(MDIM,MDIM),X2(MDIM,MDIM),TEMPV(MDIM),TEMP
  STORE ROW I OF X1 IN TEMPV.
  DO 4 I=1,N
    DO 1 J=1,N
      1 TEMPV(J) = X1(I,J)
      MULTIPLY COLUMN J OF X2 BY ROW I OF X1 AND STORE IN X1(I,J).
    DO 3 J=1,N
      TEMP = (ODO,ODO)
    DO 2 K=1,N
      2 TEMP = TEMP+TEMPV(K)*X2(K,J)
    3 X1(I,J) = TEMP
  4 CONTINUE
  RETURN
  END

```





```

C      DO 1 J=1,N
C      DO 1 I=1,N
C      AR(I,J) = A(1,I,J)
C      1 AI(I,J) = A(2,I,J)
C      RETURN
C      END
C      SUBROUTINE EBALAC (AR,AI,N,IA,K,L,D)
C      EBALAC-----D-----LIBRARY 1-----
C      FUNCTION
C      USAGE
C      PARAMETERS      AR
C                      AI
C                      N
C                      IA
C                      K
C                      L
C                      D
C      PRECISION
C      LANGUAGE
C      LATEST REVISION      - MARCH 9, 1977
C      SUBROUTINE EBALAC (AR,AI,N,IA,K,L,D)
C      DIMENSION      AR(IA,1),AI(IA,1),D(N)

```

DSPL 490  
 DSPL 500  
 DSPL 510  
 DSPL 520  
 DSPL 530  
 DSPL 540  
 DSPL 550  
 DSPL 560  
 DSPL 570  
 DSPL 580

EBAC0010  
 EBAC0020  
 EBAC0030  
 EBAC0040  
 EBAC0050  
 EBAC0060  
 EBAC0070  
 EBAC0080  
 EBAC0090  
 EBAC0100  
 EBAC0110  
 EBAC0120  
 EBAC0130  
 EBAC0140  
 EBAC0150  
 EBAC0160  
 EBAC0170  
 EBAC0180  
 EBAC0190  
 EBAC0200  
 EBAC0210  
 EBAC0220  
 EBAC0230  
 EBAC0240  
 EBAC0250  
 EBAC0260  
 EBAC0270  
 EBAC0280  
 EBAC0290  
 EBAC0300  
 EBAC0310  
 EBAC0320  
 EBAC0330  
 EBAC0340  
 EBAC0350  
 EBAC0360

- BALANCES A COMPLEX GENERAL MATRIX AND ISOLATES  
 EIGENVALUES WHENEVER POSSIBLE.  
 - CALL EBALAC (AR,AI,N,IA,K,L,D)  
 - INPUT/OUTPUT MATRICES OF DIMENSION N BY N.  
 ON INPUT, AR AND AI CONTAIN THE REAL  
 AND IMAGINARY PARTS, RESPECTIVELY, OF  
 THE COMPLEX MATRIX OF ORDER N TO BE  
 BALANCED. ON OUTPUT, AR AND AI CONTAIN THE  
 REAL AND IMAGINARY PARTS OF THE  
 TRANSFORMED MATRIX.  
 - INPUT VARIABLE CONTAINING THE ORDER  
 OF THE MATRIX A = (AR,AI) TO BE BALANCED.  
 - INPUT VARIABLE CONTAINING THE ROW DIMENSION OF  
 AR AND AI IN THE CALLING PROGRAM.  
 - OUTPUT INTEGERS CONTAINING THE BOUNDARY  
 INDICES FOR THE BALANCED MATRIX A = (AR,AI)  
 SUCH THAT  
 AR(I,J) = 0. AND AI(I,J) = 0. IF  
 (1) J IS GREATER THAN J AND  
 (2) J = 1,...,K-1 OR  
 I = 1,...,N  
 - OUTPUT VECTOR OF LENGTH N CONTAINING  
 INFORMATION DETERMINING THE PERMUTATIONS  
 USED AND THE SCALING FACTORS.  
 - SINGLE/DOUBLE  
 - FORTRAN

```

C          LOGICAL          NOCONV          RADIX IS A MACHINE DEPENDENT
C          DOUBLE PRECISION  AR, AI, D, RADIX, ZERO, ONE, PT95, B2, F, C, G, R, S
C          DOUBLE PRECISION  RRADIX, RB2
C          DATA             RADIX/16.0D0/
C          DATA             ZERO, ONE, PT95/0.0D0, 1.0D0, 0.95D0/
C          B2 = RADIX*RRADIX
C          RRADIX = ONE/RADIX
C          RB2 = RRADIX*RRADIX
C          K = 1
C          L = N
C          GO TO 30
C
C          5 D(M) = J.EQ.M) GO TO 20
C          IF (J.I.EQ.1,L) GO TO 20
C          F = AR(I,J)
C          AR(I,J) = AR(I,M)
C          AR(I,M) = F
C          F = AI(I,J)
C          AI(I,J) = AI(I,M)
C          AI(I,M) = F
C          10 CONTINUE
C          DO 15 I=K,N
C          F = AR(J,I)
C          AR(J,I) = AR(M,I)
C          AR(M,I) = F
C          F = AI(J,I)
C          AI(J,I) = AI(M,I)
C          AI(M,I) = F
C          15 CONTINUE
C          20 GO TO (25,45), IEXC
C
C          25 IF (L.EQ.1) GO TO 115
C          L = L-1
C
C          30 L1 = L+1
C          DO 40 JJ = 1,L
C          J = L1-JJ
C          DO 35 I = 1,L
C          IF (I.EQ.J) GO TO 35
C          IF (AR(J,I).NE.ZERO.OR. AI(J,I).NE.ZERC) GO TO 40
C          35 CONTINUE
C
C          SEARCH FOR ROWS ISOLATING AN
C          EIGENVALUE AND PUSH THEM DOWN
C          DO J=L,1,-1

```

```

EBAC0370
EBAC0380
EBAC0390
EBAC0400
EBAC0410
EBAC0420
EBAC0430
EBAC0440
EBAC0450
EBAC0480
EBAC0490
EBAC0500
EBAC0510
EBAC0520
EBAC0530
EBAC0540
EBAC0550
EBAC0560
EBAC0570
EBAC0580
EBAC0590
EBAC0600
EBAC0610
EBAC0620
EBAC0630
EBAC0640
EBAC0650
EBAC0660
EBAC0670
EBAC0680
EBAC0690
EBAC0700
EBAC0710
EBAC0720
EBAC0730
EBAC0740
EBAC0750
EBAC0760
EBAC0770
EBAC0780
EBAC0790
EBAC0800
EBAC0810
EBAC0820
EBAC0830
EBAC0840
EBAC0850
EBAC0860

```



EBAC 0870  
EBAC 0880  
EBAC 0890  
EBAC 0900  
EBAC 0910  
EBAC 0920  
EBAC 0930  
EBAC 0940  
EBAC 0950  
EBAC 0960  
EBAC 0970  
EBAC 0980  
EBAC 0990  
EBAC 1000  
EBAC 1010  
EBAC 1020  
EBAC 1030  
EBAC 1040  
EBAC 1050  
EBAC 1060  
EBAC 1070  
EBAC 1080  
EBAC 1090  
EBAC 1100  
EBAC 1110  
EBAC 1120  
EBAC 1130  
EBAC 1140  
EBAC 1150  
EBAC 1160  
EBAC 1180  
EBAC 1200  
EBAC 1210  
EBAC 1220  
EBAC 1230  
EBAC 1240  
EBAC 1250  
EBAC 1260  
EBAC 1270  
EBAC 1280  
EBAC 1290  
EBAC 1300  
EBAC 1310  
EBAC 1320  
EBAC 1330  
EBAC 1340  
EBAC 1350  
EBAC 1360

```

C
C
      M = L
      IEXC = 1
      GO TO 5
40 CONTINUE
   GO TO 50
C
45 K = K+1
50 DO 60 J = K,L
   DO 55 I = K,L
    IF (I.EQ. J) GC TO 55
    IF (AR(I,J) .NE. ZERO .OR. AI(I,J) .NE. ZERO) GO TO 60
55 CONTINUE
   M = K
   IEXC = 2
   GO TO 5
60 CONTINUE
C
      DO 65 I = K,L
      D(I) = ONE
65 CONTINUE
C
70 NOCONV = .FALSE.
   DO 110 I = K,L
    C = ZERO
    R = ZERO
    DO 75 J = K,L
     IF (J.EQ. I) GO TO 75
     C = C+DABS(AR(J,I))+DABS(AI(J,I))
     R = R+DABS(AR(I,J))+DABS(AI(I,J))
75 CONTINUE
    G = R*RRADIX
    F = ONE
    IF (C.C+R) GO TO 85
    F = F*RRADIX
    C = C*B2
    GO TO 80
85 G = R*RRADIX
90 IF (C.LT. G) GO TO 95
    F = F*RRADIX
    C = C*RB2
    GO TO 90
C
95 IF ((C+R)/F .GE. PT95*S) GO TO 110
   G = ONE/F
   D(I) = D(I)*F
      BALANCE
      GO TO 110

```

EBAC1370  
EBAC1380  
EBAC1390  
EBAC1400  
EBAC1410  
EBAC1420  
EBAC1430  
EBAC1440  
EBAC1450  
EBAC1460  
EBAC1470  
EBAC1480  
EBAC1490  
EHEC0010  
EHEC0020  
EHEC0030  
EHEC0040  
EHEC0050  
EHEC0060  
EHEC0070  
EHEC0080  
EHEC0090  
EHEC0100  
EHEC0110  
EHEC0120  
EHEC0130  
EHEC0140  
EHEC0150  
EHEC0160  
EHEC0170  
EHEC0180  
EHEC0190  
EHEC0200  
EHEC0210  
EHEC0220  
EHEC0230  
EHEC0240  
EHEC0250  
EHEC0260  
EHEC0270  
EHEC0280  
EHEC0290  
EHEC0300  
EHEC0310  
EHEC0320  
EHEC0330  
EHEC0340





EHEC0870  
EHEC0880  
EHEC0890  
EHEC0900  
EHEC0910  
EHEC0920  
EHEC0930  
EHEC0940  
EHEC0970  
EHEC0950  
EHEC0980  
EHEC0960  
EHEC0990  
EHEC1000  
EHEC1010  
EHEC1020  
EHEC1030  
EHEC1040  
EHEC1050  
EHEC1060  
EHEC1070

```

20 IF (XR .EQ. ZERO .AND. XI .EQ. ZERO) GO TO 40
   MP1=M+1
   DO 35 I=MP1,L
     YR=AR(I,M-1)
     YI=AI(I,M-1)
     IF (YR .EQ. ZERO .AND. YI .EQ. ZERO) GO TO 35
     Y=Y/X
     AR(I,M-1)=YR
     AI(I,M-1)=YI
     AI(I,J)=AI(I,J)-YR*AI(M,J)-YI*AR(M,J)
     DO 25 J=M,N
       CONTINUE
     DO 30 J=1,L
       AR(J,M)=AR(J,M)+YR*AR(J,I)-YI*AI(J,I)
       AI(J,M)=AI(J,M)+YI*AR(J,I)-YR*AI(J,I)
       CONTINUE
     CONTINUE
   CONTINUE
30 CONTINUE
35 CONTINUE
40 RETURN
45 END

```

```

CCCCCCCCCCCCCCCCCCCC
C-----D-----LIBRARY 1-----
SUBROUTINE ELRH2C (HR,HI,K,L,N,IH,WR,WI,ZR,ZI,ID,INFER,IER)
FUNCTION
USAGE
PARAMETERS  FR      HI      K      L      N
- COMPUTE THE EIGENVALUES AND EIGENVECTORS OF
  A COMPLEX UPPER HESSENBERG MATRIX AND
  BACK TRANSFORM THE EIGENVECTORS.
- CALL ELRH2C (FR,HI,K,L,N,IH,WR,WI,ZR,ZI,ID,
  INFER,IER)
- INPUT MATRIX OF DIMENSION N BY N CONTAINING
  THE REAL COMPONENTS OF THE COMPLEX
  HESSENBERG MATRIX. HR IS DESTROYED ON
  OUTPUT.
- INPUT MATRIX OF DIMENSION N BY N CONTAINING
  THE IMAGINARY COUNTERPARTS TO HR, ABOVE.
  HI IS DESTROYED ON OUTPUT.
- INPUT SCALAR CONTAINING THE LOWER BOUNDARY
  INDEX FOR THE INPUT MATRIX.
- INPUT SCALAR CONTAINING THE UPPER BOUNDARY
  INDEX FOR THE INPUT MATRIX.
- INPUT SCALAR CONTAINING THE ORDER OF THE
  HESSENBERG MATRIX AND THE EIGENVECTOR
  MATRIX.
ELRH2C-----
ELR20010
ELR20020
ELR20030
ELR20040
ELR20050
ELR20060
ELR20070
ELR20080
ELR20090
ELR20100
ELR20110
ELR20120
ELR20130
ELR20140
ELR20150
ELR20160
ELR20170
ELR20180
ELR20190
ELR20200
ELR20210
ELR20220
ELR20230
ELR20240
ELR20250

```

AD-A066 374

NAVAL POSTGRADUATE SCHOOL MONTEREY CALIF  
INVESTIGATION OF PIPE FLOW INSTABILITY AND RESULTS FOR WAVE NUM--ETC(U)  
DEC 78 M J ARNOLD

F/G 20/4

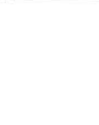
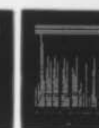
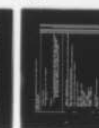
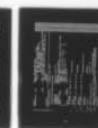
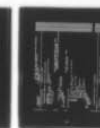
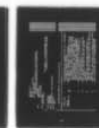
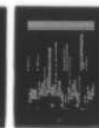
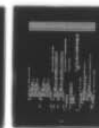
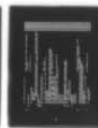
NUM--ETC(U)

UNCLASSIFIED

NL

2 OF 2

AD  
A066374



END  
DATE  
FILMED

'5--79  
DDC

```

CCCCCCCCCCCCCCCCCCCCCCCCCCCCCCCCCCCCCCCCCCCCCCCCCCCCCCCCCCCC
IH      - INPUT SCALAR CONTAINING THE ROW DIMENSION
        OF MATRICES HR, HI, ZR AND ZI IN THE
        CALLING PROGRAM.
WR      - OUTPUT VECTOR OF THE EIGENVALUES.
WI      - COMPONENTS OF LENGTH N CONTAINING THE REAL
        OUTPUT VECTOR OF LENGTH N CONTAINING THE
        IMAGINARY COMPONENTS OF THE EIGENVALUES.
ZR      - OUTPUT MATRIX OF DIMENSION N BY N CONTAINING
        THE REAL COMPONENTS OF THE EIGENVECTORS.
ZI      - THE EIGENVECTORS ARE NOT NORMALIZED.
        OUTPUT MATRIX OF DIMENSION N BY N CONTAINING
        THE IMAGINARY COMPONENTS TO ZR, ABOVE.
ID      - INPUT VECTOR OF LENGTH N CONTAINING THE
        INFORMATION GENERATED BY IMSL ROUTINE
        HESSENBERG IDENTIFYING THE ROWS AND COLUMNS
        INTERCHANGED DURING THE REDUCTION TO
        HESSENBERG FORM. ONLY COMPONENTS K
        THROUGH L ARE USED.
INFER   - OUTPUT SCALAR CONTAINING THE INDEX OF THE
        EIGENVALUE WHICH GENERATED THE TERMINAL
        ERROR (SEE DESCRIPTION OF IER, BELOW).
IER      - ERROR PARAMETER
        TERMINAL ERROR = 128 + N
        N = 1 INDICATES THE EIGENVALUE RECORDED
        IN THE OUTPUT PARAMETER, INFER,
        COULD NOT BE DETERMINED AFTER 30
        ITERATIONS. IF THE J-TH EIGENVALUE
        COULD NOT BE SO DETERMINED,
        THEN THE EIGENVALUES J+1, J+2, ..., N
        SHOULD BE CORRECT.

PRECISION  - SINGLE/DOUBLE
REQD. IMSL  - UERTST
LANGUAGE    - FORTRAN

LATEST REVISION - APRIL 5, 1977

SUBROUTINE ELRH2C (HR, HI, K, L, N, IH, WR, WI, ZR, ZI, ID, INFER, IER)
DIMENSION
COMPLEX*16
DOUBLE PRECISION
DOUBLE PRECISION
DOUBLE PRECISION
EQUIVALENCE
1
2 DATA

```

```

ELR20260
ELR20270
ELR20280
ELR20290
ELR20300
ELR20310
ELR20320
ELR20330
ELR20340
ELR20350
ELR20360
ELR20370
ELR20380
ELR20390
ELR20400
ELR20410
ELR20420
ELR20430
ELR20440
ELR20450
ELR20460
ELR20470
ELR20480
ELR20490
ELR20500
ELR20510
ELR20520
ELR20530
ELR20540
ELR20550
ELR20560
ELR20570
ELR20580
ELR20590
ELR20600
ELR20610
ELR20620
ELR20630
ELR20640
ELR20650
ELR20660
ELR20680
ELR20690
ELR20700
ELR20710
ELR20720
ELR20730
ELR20740

```



ELR20750  
ELR20770  
ELR20780  
ELR20790  
ELR20800  
ELR20810  
ELR20820  
ELR20830  
ELR20840  
ELR20850  
ELR20860  
ELR20870  
ELR20880  
ELR20890  
ELR20900  
ELR20910  
ELR20920  
ELR20930  
ELR20940  
ELR20950  
ELR20960  
ELR20970  
ELR20980  
ELR20990  
ELR21000  
ELR21010  
ELR21020  
ELR21030  
ELR21040  
ELR21050  
ELR21060  
ELR21070  
ELR21080  
ELR21090  
ELR21100  
ELR21110  
ELR21120  
ELR21130  
ELR21140  
ELR21150  
ELR21160  
ELR21170  
ELR21180  
ELR21190  
ELR21200  
ELR21210  
ELR21220  
ELR21230

```

C      DATA
      EPS/Z3410000000000000000/
      INITIALIZE IER

      IER=0
      INFER=0
      TR=ZERO
      TI=ZERO
      DC 5 I=1,N
      DO 3 J=1,N
        ZR(I,J)=ZERO
        ZI(I,J)=ZERO
      3 CONTINUE
      ZR(I,I) = ONE
      5 CONTINUE

      FORM THE MATRIX OF ACCUMULATED
      TRANSFORMATIONS FROM THE INFOR-
      MATION LEFT BY ROUTINE 'EHESSC'

      IEND=L-K-1
      IF (IEND .LE. 0) GO TO 25
      DO 20 I=1,IEND
        I=L-I
        IP1=I+1
        IM1=I-1
        DO 10 M=IP1,L
          ZR(M,I)=HR(M,IM1)
          ZI(M,I)=HI(M,IM1)
        10 CONTINUE
        J=I+1
        IF (I .EQ. J) GO TO 20
        DO 15 M=I,L
          ZR(I,M)=ZR(J,M)
          ZI(I,M)=ZI(J,M)
          ZR(J,M)=ZERO
          ZI(J,M)=ZERO
        15 CONTINUE
        ZR(J,I)=ONE
        20 CONTINUE
        DO 25 I=1,N
          IF (I .GE. K .AND. I .LE. L) GO TO 30
          WR(I)=HR(I,I)
          WI(I)=HI(I,I)
        25 CONTINUE
        NN=L
        30 CONTINUE
        SEARCH FOR NEXT EIGENVALUE

        35 IF (NN .LT. K) GO TO 150
        ITS=0
        NNM1=NN-1
        NNM2=NN-2

```

```

C      IF (NN .EQ. K) GO TO 50
C      LOOK FOR SINGLE SMALL SUB-DIAGONAL
C      ELEMENT
C      DO M=NN,K+1,-1
C      DO 45 KK=K,NNM1
C      M=NPL-KK
C      MM1=M-1
C      IF (DABS(HR(M,MM1))+DABS(HI(M,MM1))) .LE. EPS*(DABS(HR(MM1,MM1))) GO TO 55
C      IF +DABS(HI(MM1,MM1))+DABS(HR(M,M)))+DABS(HI(M,M))) GO TO 55
C      1 CONTINUE
C      45 M=K
C      55 IF (M .EQ. NN) GO TO 145
C      IF (ITS .EQ. 30) GO TO 205
C      IF (ITS .EQ. 10 .OR. ITS .EQ. 20) GO TO 60
C      SR=HR(NN,NN)
C      SI=HI(NN,NN)
C      XR=HR(NN,NN)*HR(NN,NNM1)-HI(NN,NN)*HI(NN,NNM1)
C      XI=HR(NN,NNM1)*HI(NN,NNM1)+HI(NN,NNM1)*HR(NN,NNM1)
C      IF (XR .EQ. ZERO .AND. XI .EQ. ZERO) GO TO 65
C      YI=(HR(NN,NNM1)-SI)/TWO
C      YI=(HI(NN,NNM1)-SI)/TWO
C      Z=CDSQRT(DCMPLX(YR**2-YI**2+XR,TWO*YR*YI+XI))
C      IF (YR**2+YI**2 .LT. ZERO) Z=-Z
C      X=X/(Y+Z)
C      SR=SR-XR
C      SI=SI-XI
C      GO TO 65
C      60 SR=DABS(HR(NN,NNM1))+DABS(HR(NN,NNM1,NNM2))
C      SI=DABS(HI(NN,NNM1))+DABS(HI(NN,NNM1,NNM2))
C      65 DO 70 I=K,NN
C      HR(I,I)=HR(I,I)-SR
C      HI(I,I)=HI(I,I)-SI
C      70 CONTINUE
C      TR=TR+SR
C      TI=TI+SI
C      ITS=ITS+1
C      XR=DABS(HR(NN,NNM1,NNM1))+DABS(HI(NN,NNM1,NNM1))
C      YR=DABS(HR(NN,NNM1))+DABS(HI(NN,NNM1))
C      ZR=DABS(HR(NN,NNM1))+DABS(HI(NN,NNM1))
C      NNMJ=NNM1-M
C      IF (NNMJ .EQ. 0) GO TO 80
C      DO MM=NN-1,M+1,-1
C      DO 75 NM=1,NNMJ
C      PM=NN-NM
C      LOOK FOR TWO CONSECUTIVE SMALL
C      SUB-DIAGONAL ELEMENTS
C      75 NM=1,NNMJ
C      PM=NN-NM

```

```

ELR21240
ELR21250
ELR21260
ELR21270
ELR21280
ELR21290
ELR21300
ELR21310
ELR21320
ELR21330
ELR21360
ELR21370
ELR21380
ELR21390
ELR21400
ELR21410
ELR21420
ELR21430
ELR21440
ELR21450
ELR21460
ELR21470
ELR21480
ELR21490
ELR21510
ELR21520
ELR21530
ELR21540
ELR21550
ELR21560
ELR21570
ELR21600
ELR21610
ELR21620
ELR21630
ELR21640
ELR21650
ELR21660
ELR21670
ELR21680
ELR21690
ELR21700
ELR21710
ELR21750
ELR21760
ELR21770
ELR21780
ELR21790

```



ELR21800  
ELR21810  
ELR21820  
ELR21840  
ELR21850  
ELR21860  
ELR21880  
ELR21890  
ELR21900  
ELR21910  
ELR21920  
ELR21930  
ELR21940  
ELR21950  
ELR21960  
ELR21970  
ELR21980  
ELR21990  
ELR22010  
ELR22020  
ELR22030  
ELR22040  
ELR22050  
ELR22060  
ELR22070  
ELR22080  
ELR22090  
ELR22100  
ELR22110  
ELR22120  
ELR22130  
ELR22140  
ELR22150  
ELR22160  
ELR22170  
ELR22180  
ELR22190  
ELR22200  
ELR22210  
ELR22220  
ELR22230  
ELR22240  
ELR22250  
ELR22260  
ELR22270  
ELR22280  
ELR22290  
ELR22300

```

MMMI=MM-1
YI=YR
YR=DABS(HR(MM,MMMI))+DABS(HI(MM,MMMI))
XI=ZXR
ZXR=XR
XR=DABS(HR(MMMI,MMMI))+DABS(HI(MMMI,MMMI))
IF (YR .LE. EPS*ZXR/YI*(ZXR+XR+XI)) GO TO 85
75 CONTINUE
80 MM=M
C
85 MP1=MM+1
DO 110 I=MP1,NN
  IM1=I-1
  XR=HR(IM1,IM1)
  XI=HI(IM1,IM1)
  YR=HR(I,IM1)
  YI=HI(I,IM1)
  IF (DABS(XR)+DABS(XI) .GE. DABS(YR)+DABS(YI)) GO TO 95
  INTERCHANGE ROWS OF HR AND HI
  DO 90 J=IM1,N
    ZZR=HR(IM1,J)
    HR(IM1,J)=HR(I,J)
    HR(I,J)=ZZR
    ZZI=HI(IM1,J)
    HI(IM1,J)=HI(I,J)
    HI(I,J)=ZZI
  CONTINUE
  Z=X/Y
  WR(I)=ONE
  GO TO 100
  Z=Y/X
  WR(I)=-ONE
  HR(I,IM1)=ZZR
  HI(I,IM1)=ZZI
  DO 105 J=I,N
    HR(I,J)=HR(I,J)-ZZR*HR(IM1,J)+ZZI*HI(IM1,J)
    HI(I,J)=HI(I,J)-ZZR*HI(IM1,J)-ZZI*HR(IM1,J)
  CONTINUE
105 CONTINUE
110 CONTINUE
C
DO 140 J=MP1,NN
  JM1=J-1
  XR=HR(J,JM1)
  XI=HI(J,JM1)
  HR(J,JM1)=ZERO
  HI(J,JM1)=ZERO
C
INTERCHANGE COLUMNS OF HR, HI,
ZR, AND ZI IF NECESSARY
COMPOSITION R*L=H
TRIANGULAR DECOMPOSITION H=L*R

```



ELR222310  
ELR222320  
ELR222330  
ELR222340  
ELR222350  
ELR222360  
ELR222370  
ELR222380  
ELR222390  
ELR222400  
ELR222410  
ELR222420  
ELR222430  
ELR222440  
ELR222450  
ELR222460  
ELR222470  
ELR222480  
ELR222490  
ELR222500  
ELR222510  
ELR222520  
ELR222530  
ELR222540  
ELR222550  
ELR222560  
ELR222570  
ELR222580  
ELR222590  
ELR222600  
ELR222610  
ELR222620  
ELR222630  
ELR222640  
ELR222650  
ELR222660  
ELR222670  
ELR222680  
ELR222690  
ELR222700  
ELR222710  
ELR222720  
ELR222730  
ELR222740  
ELR222750  
ELR222760  
ELR222780  
ELR222790  
ELR222800

```

IF (WR(J).LE. ZERC) GO TO 125
DO 115 I=1,J
  ZZR=HR(I,JM1)
  HR(I,JM1)=HR(I,J)
  HR(I,J)=ZZR
  ZZI=HI(I,JM1)
  HI(I,JM1)=HI(I,J)
  HI(I,J)=ZZI
CONTINUE
DO 120 I=K,L
  ZZR=ZR(I,JM1)
  ZR(I,JM1)=ZR(I,J)
  ZR(I,J)=ZZR
  ZZI=ZI(I,JM1)
  ZI(I,JM1)=ZI(I,J)
  ZI(I,J)=ZZI
CONTINUE
C 120
C 125 DO 130 I=1,J
  HR(I,JM1)=HR(I,JM1)+XR*HR(I,J)-XI*HI(I,J)
  HI(I,JM1)=HI(I,JM1)+XR*HI(I,J)+XI*HR(I,J)
CONTINUE
C 130
C 135 DO 135 I=K,L
  ZR(I,JM1)=ZR(I,JM1)+XR*ZR(I,J)-XI*ZI(I,J)
  ZI(I,JM1)=ZI(I,JM1)+XR*ZI(I,J)+XI*ZR(I,J)
CONTINUE
C 135
C 140 CONTINUE
GC TO 40
C 145 WR(NN)=HR(NN,NN)+TR
  WI(NN)=HI(NN,NN)+TI
  NN=NNM1
GO TO 35
C 150 IF (N.EQ. 1) GO TO 9005
  FNORM=ZERO
  DC 160 I=1,N
  FNORM=FNORM+DABS(WR(I))+DABS(WI(I))
  IF (I.EQ. N) GO TO 160
  IP1=I+1
  DO 155 J=IP1,N
    FNORM=FNORM+DABS(HR(I,J))+DABS(HI(I,J))
  CONTINUE
CONTINUE
C 155
C 160 IF (FNORM.EQ. ZERO) GO TO 9005
  ALL ROOTS FOUND. BACKSUBSTITUTE TO
  FIND VECTORS OF UPPER TRIANGULAR
  FORM

```

101



ELR23290  
ELR23300  
ELR23310  
ELR23320  
ELR23330  
ELR23340  
ELR23350  
ELR23360  
ELR23370  
ELR23380  
ELR23390  
ELR23400  
ELR23410  
ELR23420  
ELR23430  
ELR23440  
ELR23450  
ELR23460  
ELR23470

```

ZZI=ZI(I,J)
MM=JMI
IF (L.LT.J) MM=L
DO 195 M=K,MM
  ZZR=ZZR+ZR(I,M)*HR(M,J)-ZI(I,M)*HI(M,J)
  ZZI=ZZI+ZR(I,M)*HI(M,J)+ZI(I,M)*HR(M,J)
195 CONTINUE
  ZR(I,J)=ZZR
  ZI(I,J)=ZZI
200 CONTINUE
  GO TO 9005
C
205 IER=129
  INFER=NN
9000 CONTINUE
  CALL UERTST (IER,6HELRH2C)
9005 RETURN
END

```

SET ERROR - NO CONVERGENCE TO AN  
EIGENVALUE AFTER 30 ITERATIONS

EBBC0010  
EBBC0020  
EBBC0030  
EBBC0040  
EBBC0050  
EBBC0060  
EBBC0070  
EBBC0080  
EBBC0090  
EBBC0100  
EBBC0110  
EBBC0120  
EBBC0130  
EBBC0140  
EBBC0150  
EBBC0160  
EBBC0170  
EBBC0180  
EBBC0190  
EBBC0200  
EBBC0210  
EBBC0220  
EBBC0230  
EBBC0240  
EBBC0250  
EBBC0260  
EBBC0270

```

SUBROUTINE EBBCKC (ZR,ZI,N,IZ,K,L,M,D)
-----LIBRARY 1-----
FUNCTION
USAGE
PARAMETERS
  ZR
  ZI
  N
  IZ
  K
  L
  M
  D

```

- BACKTRANSFORM THE EIGENVECTORS OF A BALANCED COMPLEX GENERAL MATRIX.
- CALL EBBCKC (ZR,ZI,N,IZ,K,L,M,D)
- INPUT/OUTPUT MATRICES OF DIMENSION N BY M. ON INPUT, THE FIRST M COLUMNS OF ZR AND ZI CONTAIN THE REAL AND IMAGINARY PARTS, RESPECTIVELY, OF THE EIGENVECTORS TO BE BACK TRANSFORMED. ON OUTPUT, THESE M COLUMNS CONTAIN THE REAL AND IMAGINARY PARTS OF THE TRANSFORMED EIGENVECTORS.
- INPUT SCALAR CONTAINING THE NUMBER OF ROWS IN THE MATRIX Z = (ZR,ZI). N MUST NOT BE GREATER THAN IZ.
- INPUT SCALAR CONTAINING THE ROW DIMENSION OF MATRICES ZR AND ZI IN THE CALLING PROGRAM.
- INPUT SCALARS CONTAINING THE BOUNDARY INDICES FOR THE BALANCED MATRIX. K AND L ARE TWO OUTPUT PARAMETERS FROM IMSL ROUTINE EBALAC.
- INPUT SCALAR CONTAINING THE NUMBER OF COLUMNS OF Z = (ZR,ZI) TO BE BACK TRANSFORMED.
- INPUT VECTOR OF LENGTH N CONTAINING THE







```
//EIG$FCN JOB (1719,0947,AX74), 'SMC 1882', TIME=2  
//EXEC FORTCLGW  
//FORT.SYSIN DD *  
.....  
PROGRAM EIGFCN  
  
PERTURBATION VELOCITY PLOT PROGRAM  
  
NI = 0  
  
PURPOSE  
  
TO PLOT THE NONDIMENSIONALIZED PERTURBATION VELOCITY U AGAINST  
NONDIMENSIONALIZED RADIUS UTILIZING THE DATA GENERATED  
BY PROGRAM PIPEO (MODE=1). PLOTTING IS PERFORMED ON  
THE NPS VERSATEC PLOTTER USING SUBROUTINE PLOTG.  
  
.....  
  
IMPLICIT REAL*8(A-H,O-Z)  
COMPLEX *16QPRIM(85),DQPRM(85),ALPHA,UP(85),UPPRIM(85),CONST,GAMMA  
  
1A REAL *8ETA(85),U(85),UR(85),UI(85)  
REAL *4URI(85),UII(85),RADI(85),SREY,SLAMDA,SGAMMA,AR,AI  
  
READ N,REY,ALPHA,LAMBDA,GAMMA & QPRIME'S  
  
READ (5,6) N,REY,ALPHA  
NO = N+1  
NI = N+2  
READ (5,7) AMDA,GAMMA  
READ (5,8) KSET  
SLAMDA = AMDA  
SREY = REY  
AR = ALPHA  
AI = AIMAG(ALPHA)  
SGAMMA = GAMMA  
SGAMMA = SGAMMA + AR  
  
DC 1 I=2,NO  
READ (5,9) ETA(I),QPRIM(I)  
CONTINUE
```



```

C      C
C      COMPUTE UPPRIME'S
C      DEL = 1.00/DFLOAT (N+1)
C      ETA(1) = 0.000
C      QPRIM(1) = 1.79591836700*QPRIM(2)-1.2478134100*QPRIM(3)+0.60641399
C      1400*QPRIM(4)-0.17784256600*QPRIM(5)+0.02332361500*QPRIM(6)
C      UPPRIM(1) = 2.00*QPRIM(1)
C      CALL COEFNT (ETA(2), AMDA, COEF, KSET)
C      DQPRIM(2) = 2.00*(-QPRIM(2)+QPRIM(3))/(3.00*DEL)
C      DQPRIM(2) = COEF*DQPRIM(2)
C      UPPRIM(2) = 2.00*QPRIM(2)+ETA(2)*DQPRIM(2)
C      CALL COEFNT (ETA(3), AMDA, COEF, KSET)
C      DQPRIM(3) = 4.00*(-QPRIM(2)+QPRIM(3))/(3.00*DEL)
C      DQPRIM(3) = COEF*DQPRIM(3)
C      UPPRIM(3) = 2.00*QPRIM(3)+ETA(3)*DQPRIM(3)
C      C
C      DO 2 I=4,N
C      CALL COEFNT (ETA(I), AMDA, COEF, KSET)
C      DQPRIM(I) = (QPRIM(I+1)-QPRIM(I-1))/(2.00*DEL)
C      DQPRIM(I) = COEF*DQPRIM(I)
C      UPPRIM(I) = 2.00*QPRIM(I)+ETA(I)*DQPRIM(I)
C      2 CONTINUE
C      C
C      CALL COEFNT (ETA(NO), AMDA, COEF, KSET)
C      DQPRIM(NO) = -QPRIM(N)/(2.00*DEL)
C      DQPRIM(NO) = COEF*DQPRIM(NO)
C      UPPRIM(NO) = 2.00*QPRIM(NO)+ETA(NO)*DQPRIM(NO)
C      ETA(N1) = 1.000
C      UPPRIM(N1) = (0.00,0.00)
C      WRITE (6,10)
C      DETERMINE U VECTOR OF LARGEST MAGNITUDE
C      C = 0.00
C      DO 3 I=1,N1
C      IF (CDABS(UPPRIM(I)).GT.C) INDEX=I
C      IF (CDABS(UPPRIM(I)).GT.C) C=CDABS(UPPRIM(I))
C      3 CONTINUE
C      CONST = DCONJG(UPPRIM(INDEX))/C**2

```

```

C C C C
NORMALIZE UPRIMES'S AND SPLIT INTO REAL & IMAGINARY VECTORS
DO 4 I=1,N1
  UP(I) = CONST*UPPRIM(I)
  UR(I) = UP(I)
  UI(I) = (ODO,-1DO)*UP(I)
4 CONTINUE
C C C C C
CONVERT U'S AND ETA'S TO SINGLE PRECISION FOR PLOTG
DO 5 I=1,N1
  RAD1(I) = ETA(I)
  UR1(I) = UR(I)
  UI1(I) = UI(I)
  WRITE (6,11) RAD1(I),UR1(I),UI1(I)
5 CONTINUE
C C C C C
PLOT RESULTS
CALL PLOTG(RAD1,UR1,N1,1,1,1,'RADIUS',6,'PERTURBATION VELOCITY',
$ 21,0,1,1,1,1,7,7,7)
CALL PLOTG(RAD1,UR1,N1,2,1,5,'RADIUS',6,'PERTURBATION VELOCITY',
$ 21,0,1,1,1,1,7,7,7)
CALL CHART (N,SREY,AR,AI,SGAMMA,SLAMDA)
CALL PLOT (0.0,0.0,999)
STOP
C
6 FORMAT (I2,3D20.10)
7 FORMAT (F15.7,2(1PD20.10))
8 FORMAT (I2)
9 FORMAT (F15.7,2(1PD20.10))
10 FORMAT (I1)
11 FORMAT (I1,3F15.7)
END
C C C C C C C C C C
.....SUBROUTINE COEFNT(ETA,AMDA,COEF,KSET).....COEF 10
COEF 20
COEF 30
PURPOSE--WHEN AN OFFSET MESH IS USED, THIS SUBROUTINE GENERATES
THE COEFFICIENT REQUIRED TO CONVERT DQ/DETA TO DQ/DR AND
CONVERTS THE UNIFORM ETA VALUE INTO THE NONUNIFORM R VALUE
COEF 40
COEF 50
COEF 60
COEF 70

```

EIGF 940  
EIGF 950  
EIGF 960  
EIGF 970  
EIGF 980  
EIGF 990  
EIGF 1000  
EIGF 1010  
EIGF 1020  
EIGF 1030  
EIGF 1040  
EIGF 1050  
EIGF 1060  
EIGF 1070  
EIGF 1080  
EIGF 1090  
EIGF 1100  
EIGF 1110  
EIGF 1120  
EIGF 1130  
EIGF 1140  
EIGF 1150  
EIGF 1160  
EIGF 1170  
EIGF 1180  
EIGF 1190  
EIGF 1200  
EIGF 1210  
EIGF 1220  
EIGF 1230  
EIGF 1240  
EIGF 1250  
EIGF 1260  
EIGF 1270  
EIGF 1280  
EIGF 1290  
EIGF 1300  
EIGF 1310  
EIGF 1320





```

3 COEF = 100
  RETURN
  END
.....SUBROUTINE CHART(N,SREY,AR,AI,SGAMMA,SLAMDA).....
PURPOSE
  TO LABEL THE GRAPH WITH INFORMATION PERTAINING TO THE PLOT
EXAMPLE OF THE CALLING ARGUMENT
  CALL CHART(N,SREY,AR,AI,SGAMMA,SLAMDA)
DESCRIPTION OF PARAMETERS
  THE PARAMETERS ARE SELF-EXPLANATORY AND MUST BE IN SINGLE
  PRECISION FOR PLOTTING.
OTHER SUBROUTINES NEEDED
  ONLY BUILT-IN VERSATEC PLOTTING FUNCTIONS NEWPEN,SYMBOL &
  NUMBER. NOTE THAT THESE ROUTINES MAY ONLY BE
  ACCESSED WHEN RUNNING UNDER 'FORTCLGW'.
.....
SUBROUTINE CHART (N,SREY,AR,AI,SGAMMA,SLAMDA)
  X0 = 2.5
  Y0 = 6.5
  HT = 0.15
  HT1 = 0.7*HT
  DELY1 = .08*HT
  DELY2 = .065*HT1
  DELX = .1
  GRAPH TITLE
  CALL NEWPEN (2)
  CALL SYMBOL(X0,Y0,HT,'NORMALIZED PERTURBATION VELOCITY',0.,32)

```

COEF 560  
COEF 570  
COEF 580

CHAR 10  
CHAR 20  
CHAR 30  
CHAR 40  
CHAR 50  
CHAR 60  
CHAR 70  
CHAR 80  
CHAR 90  
CHAR 100  
CHAR 110  
CHAR 120  
CHAR 130  
CHAR 140  
CHAR 150  
CHAR 160  
CHAR 170  
CHAR 180  
CHAR 190  
CHAR 200  
CHAR 210  
CHAR 220  
CHAR 230  
CHAR 240  
CHAR 250  
CHAR 260  
CHAR 270  
CHAR 280  
CHAR 290  
CHAR 300  
CHAR 310  
CHAR 320  
CHAR 330  
CHAR 340  
CHAR 350  
CHAR 360  
CHAR 370  
CHAR 380  
CHAR 390  
CHAR 400  
CHAR 410  
CHAR 420  
CHAR 430

```

XO = XO+7.*DELX
YO = YO-DELY1
CALL SYMBOL(XO,YO,HT,'FOR THE CASE N = 0',0.,18)
MESH VALUE
CALL NEWPEN(1)
XO = XO+4.*DELX
YO = YO-DELY1
SN = FLOAT(N)
CALL SYMBOL(XO,YO,HT1,'NMESH = ',0.,9)
CALL NUMBER(999.,999.,HT1,SN,0.,-1)
REY VALUE
YC = YO-DELY2
CALL SYMBOL(XO,YO,HT1,'REY = ',0.,9)
CALL NUMBER(999.,999.,HT1,SREY,0.,-1)
ALPHA VALUE
X1 = XO+11.*DELY2
YO = YO-DELY2
CALL SYMBOL(XO,YO,HT1,'ALPHA = ',0.,9)
CALL NUMBER(999.,999.,HT1,AR,0.,1)
CALL NUMBER(X1,YO,HT1,AI,0.,1)
GAMMA RL* VALUE
YO = YO-DELY2
CALL SYMBOL(XO,YO,HT1,'GAMMA* = ',0.,9)
CALL NUMBER(999.,999.,HT1,SGAMMA,0.,4)
LAMBDA VALUE
YO = YO-DELY2
CALL SYMBOL(XO,YO,HT1,'LAMBDA = ',0.,9)
CALL NUMBER(999.,999.,HT1,SLAMDA,0.,1)
SYMBOL LEGEND
YO = 1.75
CALL SYMBOL(XO,YO,HT1,'OCTAGON = U(REAL)',0.,17)
YO = YO-DELY2
CALL SYMBOL(XO,YO,HT1,'DIAMOND = U(IMAG)',0.,17)
RETURN
END

```

```

CHAR 440
CHAR 450
CHAR 460
CHAR 470
CHAR 480
CHAR 490
CHAR 500
CHAR 510
CHAR 520
CHAR 530
CHAR 540
CHAR 550
CHAR 560
CHAR 570
CHAR 580
CHAR 590
CHAR 600
CHAR 610
CHAR 620
CHAR 630
CHAR 640
CHAR 650
CHAR 660
CHAR 670
CHAR 680
CHAR 690
CHAR 700
CHAR 710
CHAR 720
CHAR 730
CHAR 740
CHAR 750
CHAR 760
CHAR 770
CHAR 780
CHAR 790
CHAR 800
CHAR 810
CHAR 820
CHAR 830
CHAR 840
CHAR 850
CHAR 860
CHAR 870
CHAR 880
CHAR 890
CHAR 900

```

```

.....
THE FOLLOWING CARDS COMPRISE THE DATA DECK FOR PROGRAM EIGFCN.
/*
//GO.SYSIN DD *
.
DATA DECK FROM ONE RUN OF PROGRAM PIPEO (MODENO = 1)
.
.
/*
.....

```





```

C      CALL SEARCH (-1,X1,Y1,NPLT1,NDIM)
C      CALL SEARCH (0,X2,Y2,NPLT2,NDIM)
C      CALL SEARCH (1,X3,Y3,NPLT3,NDIM)
C      JUMP TO PLOT LABEL ROUTINE IF NO INCIPIENT POINTS
C      IF (NPLT1) 8,8,2
C      IF POINTS COMPUTED, NEW PAGE AND WRITE THEM OUT
C      2 WRITE (6,11)
C      DC 3 I=1,NPLT1
C      WRITE (6,12) X1(I),Y1(I)
C      3 CONTINUE
C      PLOT INCIPIENT INSTABILITY POINTS
C      CALL PLOTG(X1,Y1,NPLT1,1,0,1,'ALPHA REAL',10,'ALPHA IMAGINARY',15,
C      $ XMIN,XMAX,YMIN,YMAX,7,7.)
C      LEGEND FOR INCIPIENT SYMBOL
C      CALL NEWPEN (1)
C      CALL SYMBOL (1.3,0.7,.1,'OCTAGON = INCIPIENT INSTABILITY',0.,32)
C      JUMP TO PLOT LABEL ROUTINE IF NO CRITICAL POINTS
C      IF (NPLT2) 8,8,4
C      IF POINTS COMPUTED, NEW PAGE AND PRINT THEM OUT
C      4 WRITE (6,11)
C      DO 5 I=1,NPLT2
C      WRITE (6,12) X2(I),Y2(I)
C      5 CONTINUE
C      PLOT CRITICAL POINTS
C      CALL PLOTG(X2,Y2,NPLT2,2,0,2,'ALPHA REAL',10,'ALPHA IMAGINARY',15,
C      $ XMIN,XMAX,YMIN,YMAX,7,7.)
C      LEGEND FOR CRITICAL SYMBOL

```

```

STBC 460
STBC 470
STBC 480
STBC 490
STBC 500
STBC 510
STBC 520
STBC 530
STBC 540
STBC 550
STBC 560
STBC 570
STBC 580
STBC 590
STBC 600
STBC 610
STBC 620
STBC 630
STBC 640
STBC 650
STBC 660
STBC 670
STBC 680
STBC 690
STBC 700
STBC 710
STBC 720
STBC 730
STBC 740
STBC 750
STBC 760
STBC 770
STBC 780
STBC 790
STBC 800
STBC 810
STBC 820
STBC 830
STBC 840
STBC 850
STBC 860
STBC 870
STBC 880
STBC 890
STBC 900
STBC 910
STBC 920
STBC 930

```









```

3 Y1 = G(I,J)-CRIT(NCASE,AR(I))
  Y2 = G(I,J+1)-CRIT(NCASE,AR(I))
  CALL INTERP (AI(J),AI(J+1),Y1,Y2,AIVAL)
  K = K+1
  X(K) = AR(I)
  Y(K) = AIVAL
  GO TO 5
4 X(K) = AR(I)
  Y(K) = AI(J)
5 CONTINUE

      SEARCH FOR SIGN CHANGE BY ROWS AND INTERPOLATE FOR ALPHA
      REAL AT WHICH SIGN CHANGE OCCURS

      DO 10 I=1,NDIM
      DO 10 J=1,MDIM
      IF (G(J,I)-CRIT(NCASE,AR(J))) 7,9,6
      IF (G(J+1,I)-CRIT(NCASE,AR(J+1))) 8,8,10
      IF (G(J,I)-CRIT(NCASE,AR(J)))
      Y1 = G(J,I)-CRIT(NCASE,AR(J))
      Y2 = G(J+1,I)-CRIT(NCASE,AR(J+1))
      CALL INTERP (AR(J),AR(J+1),Y1,Y2,ARVAL)
      K = K+1
      X(K) = ARVAL
      Y(K) = AI(I)
      GO TO 10
9 K = K+1
  X(K) = AR(J)
  Y(K) = AI(I)
10 CONTINUE

      RETURN
      END

.....SUBROUTINE INTERP(X1,X2,Y1,Y2,X3).....
PURPOSE
      TO LINEARLY INTERPOLATE FOR THE POINT OF ACTUAL SIGN
      CHANGE (X3) BETWEEN TWO POINTS (Y1 & Y2) OF OPPOSITE
      SIGN. THE X-COORDINATES OF Y1 & Y2 ARE X1 & X2, RESPECTIVELY.
      SAMPLE OF THE CALLING ARGUMENT

```

```

SEAR 570
SEAR 580
SEAR 590
SEAR 600
SEAR 610
SEAR 620
SEAR 630
SEAR 640
SEAR 650
SEAR 660
SEAR 670
SEAR 680
SEAR 690
SEAR 700
SEAR 710
SEAR 720
SEAR 730
SEAR 740
SEAR 750
SEAR 760
SEAR 770
SEAR 780
SEAR 790
SEAR 800
SEAR 810
SEAR 820
SEAR 830
SEAR 840
SEAR 850
SEAR 860
SEAR 870
SEAR 880
SEAR 890
SEAR 900
SEAR 910
SEAR 920
SEAR 930

INTE 10
INTE 20
INTE 30
INTE 40
INTE 50
INTE 60
INTE 70
INTE 80
INTE 90

```



CCCCCCCCCCCCCCCCCCCC	CALL INTERP(X1,X2,Y1,Y2,X3)	100	INTE
	DESCRIPTION OF PARAMETERS	110	INTE
	X1 & X2 - X-COORDINATES OF PCINTS Y1 & Y2 RESPECTIVELY.	120	INTE
	Y1 & Y2 - TWO POINTS OF OPPOSITE SIGN FOR WHICH THE POINT	130	INTE
	OF ACTUAL SIGN CHANGE (Y = 0) IS TO BE INTERPOLATED.	140	INTE
	X3 - THE VALUE OF X FOR WHICH Y = 0.	150	INTE
	OTHER ROUTINES NEEDED	160	INTE
	NONE	170	INTE
	.....	180	INTE
	SLBROUTINE INTERP (X1,X2,Y1,Y2,X3)	190	INTE
	X3 = (X2*Y1-X1*Y2)/(Y1-Y2)	200	INTE
	RETURN	210	INTE
	END	220	INTE
	.....	230	INTE
	.....	240	INTE
	.....	250	INTE
	.....	260	INTE
	.....	270	INTE
	.....	280	INTE
	.....	290	INTE
	.....	300	INTE
	.....	310	INTE
CCCCCCCCCCCCCCCCCCCC	.....BLOCK DATA.....	10	BLKD
	PURPOSE	20	BLKD
	TO INITIALIZE COMMON ARRAYS G1,AR1 & A11 TO ZERC.	30	BLKD
	SAMPLE OF CALLING ARGUMENT	40	BLKD
	NONE	50	BLKD
	DESCRIPTION OF PARAMETERS	60	BLKD
	G1 - THE MAP OF STABILITY VALUES GENERATED BY PIPEO.	70	BLKD
	EACH ELEMENT OF G1 IS A VALUE OF GAMMA* CORRESPONDING	80	BLKD
	TO A SPECIFIC VALUE OF THE REAL AND IMAGINARY PARTS OF	90	BLKD
	THE WAVE NUMBER, ALPHA.	100	BLKD
	AR1 - THE LINEAR ARRAY OF X-COORDINATES OF THE STABILITY MAP	110	BLKD
	(THE REAL PART OF THE WAVE NUMBER, ALPHA).	120	BLKD
	A11 - THE LINEAR ARRAY OF Y-COORDINATES OF THE STABILITY MAP	130	BLKD
	(THE IMAGINARY PART OF THE WAVE NUMBER, ALPHA).	140	BLKD
	OTHER ROUTINES NEEDED	150	BLKD
		160	BLKD
		170	BLKD
		180	BLKD
		190	BLKD
		200	BLKD
		210	BLKD
		220	BLKD
		230	BLKD
		240	BLKD



```

CC.....NONE.....BLKD 250
CC.....BLOCK DATA.....BLKD 260
CC.....COMMON /ARRAY/ G1(41,41),AR1(41),A11(41).....BLKD 270
CC.....DATA G1,AR1,A11/1681*0.0,82*0.0/.....BLKD 280
CC.....END.....BLKD 290
CC.....BLKD 300
CC.....BLKD 310
CC.....BLKD 320
CC.....BLKD 330

CC.....SUBROUTINE CHART(SN,SREY,SLAMDA).....CHAR 10
CC.....PURPOSE.....CHAR 20
CC.....TO LABEL THE CONTOUR PLOT.....CHAR 30
CC.....SAMPLE OF THE CALLING ARGUMENT.....CHAR 40
CC.....CALL CHART(SN,SREY,SLAMDA).....CHAR 50
CC.....DESCRIPTION OF PARAMETERS.....CHAR 60
CC.....SN - THE NUMBER OF INTERIOR MESH POINTS USED FOR THE.....CHAR 70
CC.....STABILITY CONTOUR MAP BEING PLOTTED.....CHAR 80
CC.....SREY - REYNOLDS NUMBER.....CHAR 90
CC.....SLAMDA - THE NONUNIFORM MESH PARAMETER APPLICABLE TO THE.....CHAR 100
CC.....DATA BEING PLOTTED.....CHAR 110
CC.....OTHER ROUTINES NEEDED.....CHAR 120
CC.....ONLY BUILT-IN VERSATEC PLOTTING FUNCTIONS NEWPEN,SYMBOL &.....CHAR 130
CC.....NUMBER: NOTE THAT THESE ROUTINES MAY ONLY BE ACCESSED WHEN.....CHAR 140
CC.....RUNNING UNDER 'FORTCLGW'......CHAR 150
CC.....SUBROUTINE CHART (SN,SREY,SLAMDA).....CHAR 160
CC.....X0 = 2.5.....CHAR 170
CC.....Y0 = 6.5.....CHAR 180
CC.....HT = 0.15.....CHAR 190
CC.....HT1 = 0.17*HT.....CHAR 200
CC.....DELY1 = .08*HT.....CHAR 210
CC.....DELY2 = .065*HT1.....CHAR 220
CC.....CHAR 230
CC.....CHAR 240
CC.....CHAR 250
CC.....CHAR 260
CC.....CHAR 270
CC.....CHAR 280
CC.....CHAR 290
CC.....CHAR 300
CC.....CHAR 310
CC.....CHAR 320
CC.....CHAR 330
CC.....CHAR 340
CC.....CHAR 350
CC.....CHAR 360
CC.....CHAR 370

```

CHAR 380  
CHAR 390  
CHAR 400  
CHAR 410  
CHAR 420  
CHAR 430  
CHAR 440  
CHAR 450  
CHAR 460  
CHAR 470  
CHAR 480  
CHAR 490  
CHAR 500  
CHAR 510  
CHAR 520  
CHAR 530  
CHAR 540  
CHAR 550  
CHAR 560  
CHAR 570  
CHAR 580  
CHAR 590  
CHAR 600  
CHAR 610  
CHAR 620  
CHAR 630  
CHAR 640  
CHAR 650  
CHAR 660  
CHAR 670  
CHAR 680  
CHAR 690  
CHAR 700  
CHAR 710  
CHAR 720  
CHAR 730  
CHAR 740  
CHAR 750  
CHAR 760  
CHAR 770  
CHAR 780  
CHAR 790  
CHAR 800  
CHAR 810  
CHAR 820  
CHAR 830

```

DELX = .1
GRAPH TITLE
CALL NEWPEN (2)
CALL SYMBOL(X0,Y0,HT,'STABILITY CONTOUR PLOT',0.,22)
X0 = X0+3.*DELX
YC = Y0-DELY1
CALL SYMBOL(X0,Y0,HT,'FOR THE CASE N = 0',0.,18)
MESH VA LUE
CALL NEWPEN (1)
X0 = X0+4.*DELX
Y0 = Y0-DELY1
CALL SYMBOL(X0,Y0,HT1,'NMESH = ',0.,9)
CALL NUMBER (999.,999.,HT1,SN,0.,-1)
REY VALUE
Y0 = Y0-DELY2
CALL SYMBOL(X0,Y0,HT1,'REY = ',0.,9)
CALL NUMBER (999.,999.,HT1,SREY,0.,-1)
LAMBDA VALUE
YC = Y0-DELY2
CALL SYMBOL(X0,Y0,HT1,'LAMBDA = ',0.,9)
CALL NUMBER (999.,999.,HT1,SLAMDA,0.,1)
STABILITY AREA LABELS
NOTE - SINCE THE SHAPE OF THE CURVE VARIES WITH
      EACH SET OF INPUT DATA, THE COORDINATES OF THE FOLLOWING
      LABELS MUST BE ADJUSTED FOR EACH SPECIFIC PLOT.
CALL NEWPEN (2)
CALL SYMBOL (4.0,4.5,HT1,'SUPERCRITICAL',0.,13)
CALL SYMBOL (5.6,4.5,HT1,'SUBCRITICAL',0.,11)
CALL SYMBOL (6.9,4.5,HT1,'STABLE',0.,6)
YC = 4.5-DELY2
CALL SYMBOL (4.0,Y0,HT1,'INSTABILITY',0.,12)
CALL SYMBOL (5.6,Y0,HT1,'INSTABILITY',0.,11)
RETURN
END

```

CC

CC

CC

CCC

CCCCC

C CC

```

.....
THE FOLLOWING CARDS CCMPRISE THE CATA DECK FOR PROGRAM STBCONT.
/*
//GO.SYSIN DD *
DATA DECK FROM ONE RUN OF PROGRAM PIPE0 (MODEND = 2)
.
.
/*
.....

```



### LIST OF REFERENCES

1. Davey, A., and Drazin, P.G., "The Stability of Poiseuille Flow in a Pipe," Journal of Fluid Mechanics, v. 36, part 2, p. 209, 22 August 1968.
2. Garg, V.K., and Rouleau, W.T., "Linear Spatial Stability of Pipe Poiseuille Flow," Journal of Fluid Mechanics, v. 54, part 1, p. 113, 6 January 1969.
3. Gill, A.E., "The Least-Damped Disturbance to Poiseuille Flow in a Circular Pipe," Journal of Fluid Mechanics, v. 61, part 1, p. 765, 3 December 1973.
4. Harrison, W.F., On the Stability of Poiseuille Flow, Ae. E. Thesis, Naval Postgraduate School, Monterey, California, 1975.
5. Huang, L.M. and Chen, T.S., "Stability of Developing Flow Subject to Non-axisymmetric Disturbances," Journal of Fluid Mechanics, v. 63, part 1, p. 183, 16 April 1973.
6. Johnston, R.H. III, A Program for the Stability Analysis of Pipe Poiseuille Flow, M.S. Thesis, Naval Postgraduate School, Monterey, California, 1976.
7. Leite, R.J., An Experimental Investigation of Axially Symmetric Poiseuille Flow, Report No. OSR-TR-56-2, Air Force Contract AF18(600)-350, November, 1956.
8. Naval Postgraduate School Report NPS-67Gn77051, Improved Finite Difference Formulas for Boundary Value Problems, by T.H. Gawain and R.E. Ball, 1 May 1977.
9. Naval Postgraduate School Report NPS67-78-006, A Basic Reformulation of the Pipe Flow Stability Problem and Some Preliminary Numerical Results, by T.H. Gawain, 1 September 1978.
10. Reynolds, O., "An Experimental Investigation of the Circumstances which Determine whether the Motion of Water Shall be Direct or Sinuous, and the Law of Resistance in Parallel Channels," Phil. Trans. Royal Soc., 174, p. 935-982, 1883.
11. Salwen, H., and Grosch, C.E., "The Stability of Poiseuille Flow in a Pipe of Circular Cross-section," Journal of Fluid Mechanics, v. 54, part 1, p. 93, 6 March 1972.

INITIAL DISTRIBUTION LIST

	No. Copies
1. Defense Documentation Center Cameron Station Alexandria, Virginia 22314	2
2. Library, Code 0142 Naval Postgraduate School Monterey, California 93940	2
3. Department Chairman, Code 67 Department of Aeronautics Naval Postgraduate School Monterey, California 93940	1
4. Prof. T.H. Gawain, Code 67Gn Department of Aeronautics Naval Postgraduate School Monterey, California 93940	5
5. LT Michael James Arnold, USN 10825 Single Tree Lane Spring Valley, California 92077	1